Master's Thesis of Pharmacy

TPX2 induction in long-term cultured hESCs leads to survival under mitotic stress

배양적응된 인간배아줄기세포에서 TPX2 발현 촉진에 의해 유도된 비정상 유사분열 과정에서의 생존 이점

February 2021

Graduate School of Pharmacy
Seoul National University
Pharmaceutical Biosciences **Major**

Yun-Jeong Kim

TPX2 induction in long-term cultured hESCs leads to survival under mitotic stress

지도교수 차 혁 진

이 논문을 약학석사 학위논문으로 제출함

2021년 2월

서울대학교 대학원
약학대학
의약생명과학 전공

김 윤 정

김윤정의 약학석사 학위논문을 인준함

2021년 2월

위 원 장	이 정 원	(인)
부위원장	한 병 우	(인)
위 원	차 혁 진	(인)

Abstract

For decades, there is emerging evidence that genetic alterations occur in most human embryonic stem cells (hESCs). However, considering the significance of genetic aberration of hESCs, which may arise serious safety issues for hESC based cell therapy, the molecular mechanism underlying genetic alteration has remained unclear. In particular, copy number variation (CNV) at 20q11.21 loci is one of typical genetic abnormality occurring in hESCs, implying that amplification of genes in the chromosome loci may favor the survival during long-term in vitro culture. 'Survival advantage', a typical trait acquired during long-term in vitro culture results from induction of BCL2L1 at 20q11.21. In addition, escape from mitotic cell death in the aberrant mitosis due to 'survival advantage' leads to aneuploidy. However, gene(s) to drive the genetic aberration in hESCs remains unidentified. In this study, I took advantage of a set of hESCs with different passage number to determine the putative driver of genetic aberration during mitosis. The late passage hESCs (P4) showing the clear mitotic aberration have clear CNV at 20q11.21 loci and the trait of 'survival advantage' along with induction of BCL2L1. I demonstrated that TPX2, located at 20q11.21 loci, was highly amplified in P4 hESCs. Considering role of TPX2 in not only spindle assembly

during normal mitosis but also cancer malignancy once overexpressed, TPX2 may serve as a key driver for genetic aberration in hESCs. I showed the evidence that inducible expression of TPX2 in the early passage of hESCs (P1) rescued cell death during mitotic stress. The molecular mechanism underlying TPX2 mediated mitotic survival is under being examined.

Keywords : TPX2, Survival advantage, hESCs, Aberrant mitosis, Genetic alteration

Student Number : 2019-22260

Table of Contents

List of figure

List of Table

Abbreviations

TPX2	Targeting protein for Xklp2
AURKA	Aurora kinase A
YAP	Yes-Associated Protein
TAZ	Transcriptional coactivator with PDZ-binding motif
CCLE	Cancer cell line encyclopedia
TCGA	The cancer genome atlas
MsigDB	Molecular signatures database
GEO	Gene expression omnibus
GSEA	Gene set enrichment analysis
AUC	Area under the curve
BCA	Bicinchoninic acid assay
SDS-PAGE	Sodium dodecyl sulfate - polyacrylamide gel electrophoresis
TBS	Tris-buffered saline
PVDF	Polyvinylidene fluoride
MMPs	Matrix metalloproteinases
DAPI	4’,6-diamidino-2-phenylindole

DMSO	Dimethyl sulfoxide
DMEM	Dulbecco's modified eagle medium
FBS	Fetal bovine serum

Introduction

1. Genetic aberrations in PSCs as risk factor of clinical applications

Potential of human PSCs as high proliferation and differentiation makes it possible for using PSCs as unlimited cellular source. Thus, utilization of PSC expands a lot as cellular therapy, disease modeling, toxicity test and drug discovery[1]. Large application fields of PSCs have resulted rapid progression of biological study after first human stem cell derived from human blastocyst[2]. But in other hands, risk factors of stem cell therapy have been discovered lately. The three major concerns in risk using PSCs as regenerative therapy is biodistribution, tumorigenicity and immunogenicity, which are making hurdle of diverse approach[3].

Tumorigenicity, the major technical hurdles for stem cell therapy[4], occurred by several reason, including cell of origin, genomic insertions, cell purity, and genomic integrity[3]. Several study reported about increased tumorigenicity of culture adapted PSCs[5]. Genetic abnormality ranging in size from full chromosome aneuploid to single point mutations are propagated in vitro

culture[6], and considered as the most important reason of tumorigenicity in regenerative therapy[5].

In particular, unexpected genetic mutations, identified in the induced pluripotent stem cells (iPSCs) halt the second human clinical trial of iPSC based cell therapy[7]. Genetic variants of PSCs also have the potential to cause a wide range of effects on cellular physiology that could compromise the efficacy of derivative cells used in clinical applications, or the production of such cells, or indeed the use of PSCs in research [8]. In conclusion, genetic alteration of *in vitro* PSCs is important not only in regenerative medicine, but also in research.

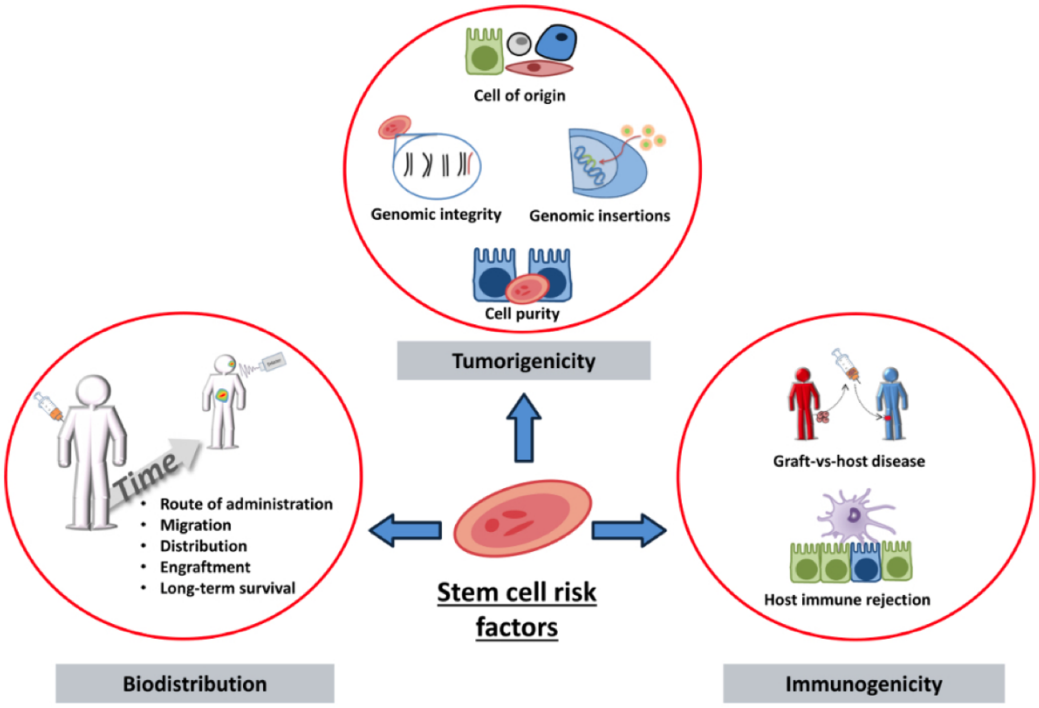

Adapted from stem cells transl. med. Apr;4(4):389-400 (2015)

Figure 1. Genetic aberrations in PSCs as risk factor of clinical application

Potential of PSCs, including embryonic stem cell(ESCs) and induced pluripotent stem cell(iPSCs) as regenerative medicine was recognized by Nobel Committee in Medicine. Three major concerns using PSCs as regenerative therapy is biodistribution, tumorigenicity and immunogenicity. Since immunogenicity problem has been overcame by SCNT(Somatic Cell Nuclear Transfer) and iPSCs, now tumorigenicity occurs by acquired genetic changes arises as a major clinical hurdle for stem cell therapy.

2. Accumulation of genetic aberration during culture

Genomic instability in hPSCs was first recognized in the early 2000s, when reports began to emerge about karyotypic abnormalities in hESCs, such as a trisomy of chromosome 12 or 17 is frequent in embryonal carcinomas [9], with following frequently mutated 20 or X chromosome. Recent studies demonstrated that aneuploid hPSCs (with trisomy in chromosome 12) show increased proliferation and impaired differentiation in vivo [10]. Until now, main reason of genetic mutation of cultured PSCs are not clearly known, while passaging during cultures are strong candidate[11]. Also aberrant mitosis, which is major reason of genetic alteration in cancer or normal cells[12], is another strong candidate as driver of genetic insufficiency in cultured PSCs.

In other side, PSCs sometimes considered as sharing cellular and molecular phenotypes with tumor cells or cancer cell lines. In specific, rapid proliferation rate, lack of contact inhibition, a propensity for genomic instability, high activity of telomerase, some high expression of oncogenes like MYC or KLF4[13] is similar. In summary, cancer cells and PSCs shows similar overall gene expression patterns. Consequently, obtain some hints from the ecology of cancer and apply it to the study of PSC have become one of strategy.

Based on the similarities between cancer and PSC discussed above, some approaches to unveil mechanisms for specific phenomenon, especially occur during the culture of PSCs[14]. Despite of methodology difference, genetic aberration accumulated in long term cultured PSCs, occasionally and rare[15]. As similar as cancer progression model, only some advantageous mutations for cell will be prevail, and during culture adaptation, characteristics as apoptotic-prone and primed mitochondria is weakened thus get survival advantage[16]. This mutation-selection hypothesis is one of the best ways to explain the culture adaptation of PSCs[8].

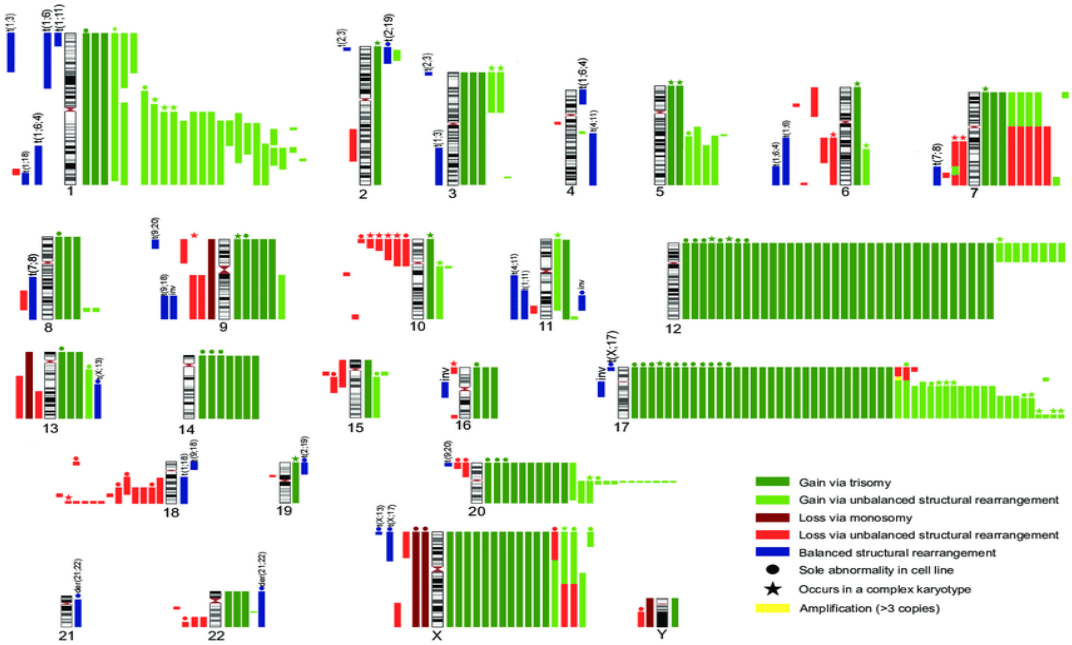

Adapted from Stem Cell Reports j Vol. 7 j 998–1012j (2016)

Figure 2. Recurrent CNV in hESCs

Genomic instability in hPSCs was began to be reported in early 2000s, such as a trisomy of chromosome 12 or 17 as well as in embryonal carcinomas, with following frequently mutated 20 or X chromosome. This genomic abnormalities, including aneuploidy results change in gene expression, proliferation and tumorigenicity. Recent studies demonstrated that aneuploid show increased proliferation and impaired differentiation in vivo.

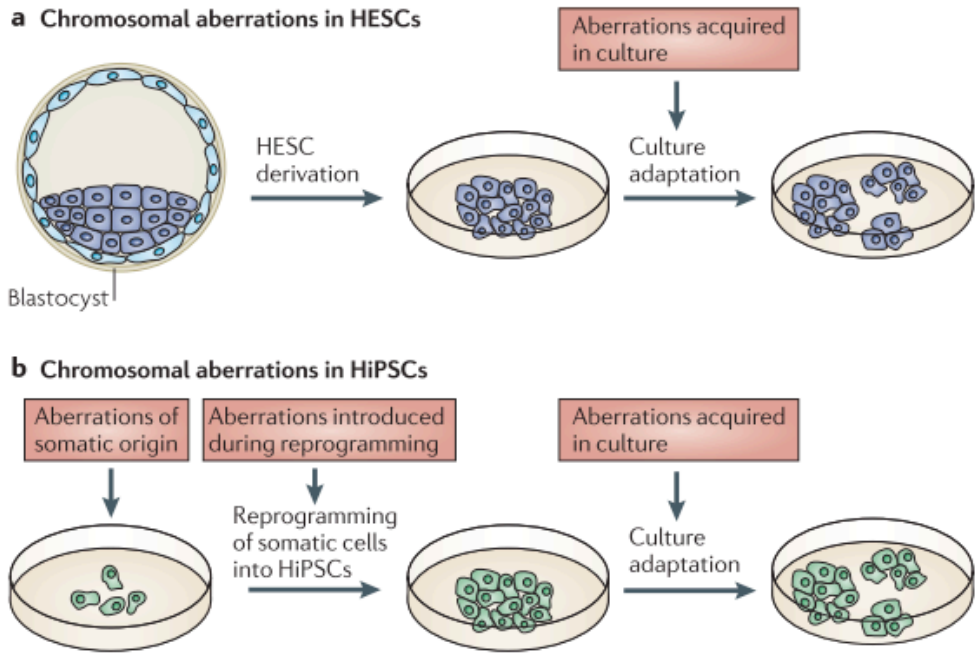

Adapted from Nat. Reviews Cancer volume 11, pages 268–277 (2011)

Figure 3. Accumulation of genetic aberration during culture

Passaging during cultures are strong candidate, while clear driver of cultural mutations are unknown. iPSCs have another source of mutation that their origin is mature somatic cells undergone multiple cell divisions and perhaps acquire aberrant genes. Because Almost mutations are selected out during first few cell divisions in culture, some genes are expected to be selected based on advantage in cell cycle profile or survival, resulting cells with culture adaptation dominant.

3. Genetic alteration and survival advantage

For decades, plenty of genetic alterations in most PSCs have been reported[17], and also mutation-selection hypothesis arose as strong candidate to explain culture adaptation of PSCs. But driver of genetic alteration in PSCs were less known. Nowadays, many clues based on massive array comparative genomic hybridization (aCGH) research is found. Most of aberration accumulated during long term culture[11] with significantly frequent aberrations in PSCs than others. Also, they become dominant very rapidly, indicating there are strong driver mutation occurs only in cultured PSCs[14]. This accumulation based on survival advantage is proved to be a cause of aneuploidy in iPSCs[18]. Intriguingly, there are several alteration fulfill all three conditions. The sub-chromosomal amplification of 20q11.21 locus, as the most frequent copy number variants (CNVs) with normal karyotype [19]. Thus, CNV of 20q11.21 does not occur in normal embryo [20]. This indicates change in *in vitro* different from embryo is related to alteration of 20q11.21. In particular, BCL2L1 in 20q11.21 loci[21], loss-of-function mutation p53[22] has been identified as a driver mutation for survival advantages in cultures.

Meanwhile, CNV including 20q11.21 loci occurs even in the early passage [23], the incidence of abnormal karyotype may take prolong culture[24]. This

suggests that induction of a set of gene(s) from CNV would lead to further chromosomal aberrations [25]. Thus, additional mechanisms rather than BCL2L1, needed to be discovered for initiation of genetic aberration. We further hypothesize that additional factor to be responsible for initiation of aneuploidy may be present at 20q.11.21 locus of which the most frequent CNV occurring in hPSCs. Specially, due to importance of normal mitosis for maintenance of genetic integrity, specific survival factor under mitotic stress would be responsible for aneuploidy formation in hPSCs.

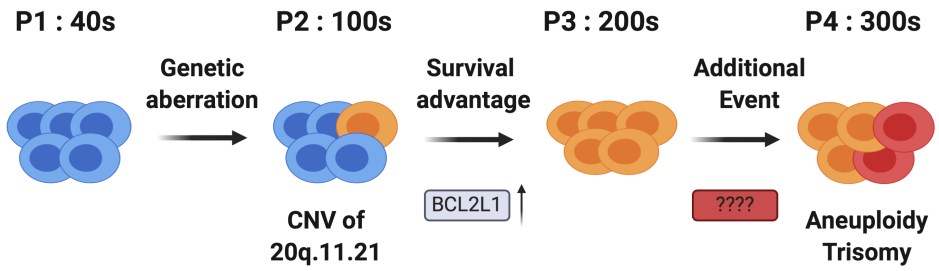

Figure 4. Two step model of aneuploidy

The sub-chromosomal amplification of 20q11.21 locus is one of the most frequent copy number variants(CNVs) only occurs in cultured hESCs, with normal karyotype, In particular, BCL2L1 in 20q11.21 loci, gives strong selective advantage due to anti-apoptotic activity. CNV including 20q11.21 loci occurs even in the early passage, but phenotype as abnormal karyotype may take time. Thus, additional mechanisms, as induction of set of gene(s) rather than BCL2L1, needed to be discovered for initiation of genetic aberration.

4. TPX2 in 20q11.21 and mitosis

Frequent mitotic error is one of key phenomenon during culture adaptation of PSCs[26] as well as major reason of genetic alteration in cancer or normal cells[12]. Thus, mitosis specific survival factor, giving survival advantage, might contributes in dominancy of cells with not only aneuploidy but also anti apoptosis. While aberrant mitosis, according to mild replication stress, is major cause of aneuploidy in cancer cells[27], mechanisms for aneuploidy in PSCs is less understood.

In the meantime, Xklp2(TPX2), localized in 20q11.21 locus with BCL2L1[19], has been studied not only in mitosis regulating microtubule length[28], nucleation, spindle assembly, ,,and centrosome separation during mitosis but also cancer[29] through activating Aurora A kinase. It controls spindle integrity, genome stability, and tumor development[30]. But in other hand, excess TPX2 interferes with microtubule disassembly and nuclei reformation at mitotic exit[31], and also cause progression of colorectal carcinoma[32].

Considering that high association of TPX2 expression to CIN in cancer [33] and to poor patient survival in various cancers[34][35], deregulation of TPX2 would be associated to driving chromosome instability through aberrant mitotic spindle dynamics and improper chromosome segregation. This line of

evidence indicates TPX2 as candidate of modulating survival advantage during mitotic stress in culture adapted PSCs. Herein, with late passage hESCs (LP-hESCs), we indicates that aberrant mitotic events such as the multipolar spindle and chromosome mis-segregation, as well as polyploidy compared to early passage hESCs (EP-hESCs), TPX2, one of the genes in 20q11.21, is identified as a putative driver for aneuploidy of hESCs through giving survival advantage against apoptosis during aberrant mitosis.

A

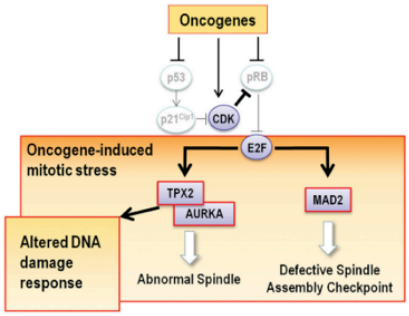

Adapted from I. De Castro et al., Genes and cancer. 2012

B

AURKA dependent	AURKA Independent
Control Mitotic spindle length/Spindle pole separation	Localizing to kinetochore
Control chromatin/kinetochore-mediated microtubule nucleation	Acquire spindle pole bipolarity
Stabilizes microtubule in prometaphase	Microtubule binding/stabilizing

Aberrated from A,Bird et al,. JCB 2009

C

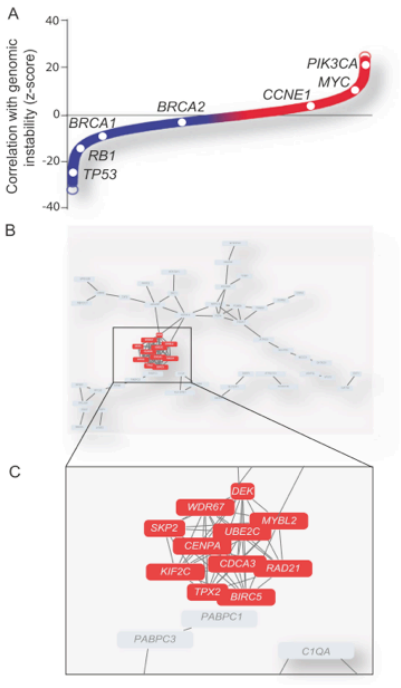

Adapted from Van Gijn et al., Oncogene, 2019

Figure 5. TPX2 in 20q11.21 and mitosis

(a)Xklp2(TPX2), localized in 20q11.21 locus with BCL2L1, is key protein in mitosis regulating microtubule nucleation, spindle assembly, and centrosome separation during mitosis. (b)Interaction of AURKA is needed for control of length of spindle, microtubule nucleation, stabilizing microtubule, but TPX2 itself also can stabilize microtubule and gives polarity to spindle pole. (c)TPX2/AURKA axis promotes 20q amplicon driven carcinoma, and is also known to be therapeutic target in genomically unstable cancer cells.

Materials and Methods

1. Reagents

The primary antibodies against α-tubulin (#sc- 8035), β-actin (#sc-47778), PARP (#sc-7150), YAP (#sc-101199) were purchased from Santa Cruz Biotechnology, Inc. Antibodies against cleaved Caspase 3 (#9661), phospho-YAP (#4911s), Smad4 (#46535), Phospho-Aurora A (#2914) were purchased from Cell Signaling Technology. Bcl-xL (ab32370) is from abcam, and Y-27632 (#1293823) was purchased from Biogems. siRNAs targeting Negative Control (#SN-1003) and the others (listed at supplement table) were obtained from Bioneer. Expression vectors of 8X GTIIC-luciferase, Flag-YAP-S94A, Myc-TEAD4, Flag-YAP-WT were kindly gifted by Prof. Mo Jung-Soon at Ajou University.

2. Cell culture

Human embryonic stem cell (WA09: H9, WiCell Research Institute, CHA3-hESCs) were maintained in iPSC-brew (Miltenyi biotechnology, #130-104-368) with 0.1% gentamycin (Gibco, Waltham, MA, USA, #15750-060) on a matrigel (Corning, Corning, NY, USA, #354277)-coated cell culture dish at 37℃ and humidifie d to 5% in a CO2 incubator. Cells were maintained with

daily changed media and passaged every 5-6 days. Upon transfer, hESCs were rinsed with DPBS and detached enzymatically with Dispase (Life Technologies) followed by 3 times washed with DMEM/F-12 (Life Technologies) media before plating. If needed 10 μM of Y27632 (Gibco) was used for cellular attachment.

3. Transfection (Plasmid DNA and siRNA)

Cells were prepared about 1 x 10^6 per 100λ in Opti-MEM. Each cell was separated to cuvettes (EC-002) with plasmid DNA 2μg (or siRNA 100pmole) added per 100λ. Electroporation was done by NEPA21 super Electroporator. After electroporation, cells were seeded to Matrigel coated culture plate with 1 μM of Y27632, and cultured for 24hr~72hr before harvest. After 24 hours, media was changed to fresh media without Y27632.

4. RNA extraction and Quantitative real time PCR

Total RNA was extracted using easy-BLUE^{TM} Total RNA Extraction Kit (#17061, iNtRON), and dissolved in RNase-free DEPC-treated water. cDNA was made using extracted RNA and RT master mix (#RR036, TAKARA). Synthesized cDNA, TB green (#RR420, TAKARA) and primers were used as

a template for examining the real-time PCR. (Primer list was shown in Table 1.) TAKARA's 2 step protocol was used by Light Cycler 480 Instrument II from Roche.

5. Immunoblotting

Cell lysates were extracted with RIPA buffer supplemented with 1% protease inhibitor cocktail and 0.1% sodium orthovanadate. After 1 hour incubation on ice, total protein was extracted by centrifuge. Concentration of total protein was quantified by BCA protein assay kit (#23225, Thermo Scientific^{TM}). Approximately 25μg of total protein were separated on various (7.5%, 10%, 15%) concentration of SDS-PAGE. Separated protein in the gel was transferred to PVDF membrane. Membrane with protein was blocked with 5% skim milk in TBS-T (Tris-buffered saline with 0.1% Tween-20) for 1 hour, and then washed by TBS-T for each 5 minutes three times. The membrane was incubated with primary antibody in TBS-T (1:1000) with 0.1% sodium azide for overnight, 4°C. Incubated membrane was washed for each 5 minutes three times with TBS-T. The membrane was incubated with HRP-conjugated secondary antibody (Jackson Immunoresearch Laboratories) in TBS-T (1:10000) for 1 hour, room temperature. Incubated membrane was washed for

each 15 minutes three times with TBS-T. Immunoreactivity was detected by Chemi-Doc using WEST-Queen^{TM} (#16026, iNtRON Biotechnology) kit.

6. Dual luciferase assay

Cells were transfected with specific promoter-luciferase vector and pRL vector using above description. Cells lysates were extracted with 1X passive lysis buffer. After 1 hour incubation on ice, total lysate was extracted by centrifuge. The supernatant was used for reaction with LARII and Stop & Glo reagent. The reporter assay was performed according to the Dual-Luciferase Reporter Assay System (#E1980, Promega).

7. Cell viability and proliferation assay

Cell death was analyzed by flow-cytometry. Regarding Annexin V/7-AAD staining, cells at 24 h after treatment of each flavonoid were washed twice with PBS and stained with FITC conjugated Annexin V antibody (BD Bioscience, Franklin Lakes, NJ, USA, #556419) and 7-AAD (BD Bioscience, #559925) or PI(Propidium iodide) for an additional 45–60 min at room temperature in the dark. Cells stained with Annexin V/7-AAD were analyzed by FACS Calibur or FACS Lyric (BD Bioscience). Concerning all of the bright field

images captured, a Light channel optical microscope (Olympus, Tokyo, Japan, CKX-41) or JULI-stage (NanoEntek, Seoul, Korea) was used in accordance with the manufacture's protocol.

8. Alkaline phosphatase (AP) assay

In order to monitor the pluripotency of hESCs, AP staining assay (Cat# 86R-1KT; Sigma-Aldrich) was performed followed by the manufacturer's instructions. Before the assay, cells were washed twice with DPBS and fixed with fixation solution (kit component).

9. G-banded karyotyping

Cells were incubated with 100ng/ml of colcemid for 2 hrs, and then collected to enrich the mitotic population. Briefly, 1% sodium citrate was slowly added for hypotonic treatment, followed by fixation with a Carnoy's solution (75% methanol and 25% acetic acid). The karyotypes were determined using a standard G-banding procedure.

10. Statistical analysis

Graphical data were presented as mean ±S.E.M. Statistical significance among three groups and between groups were determined using one- or two-way analysis of variance (ANOVA) following Bonferroni multiple comparison post-test and Student's t-test, respectively. Significance was assumed for $p<0.05$(*), $p<0.01$(**), $p<0.001$(***).

Table 1. RT-qPCR primer sequence

Gene symbol	Primer sequence (5’ to 3’)
18srRNA	F : GTA ACC CGT TGA ACC CCA TT R : CCA TCC AAT CGG TAG TAG CG
TPX2	F : GCT CAA CCT GTG CCA CAT TA R : CGA GAA AGG GCA TAT TTC CA
TPX2(KD)	F : TGG AAC AAT CCA TTC CAT CA R : AGG AGT GGC ACA TCT CTT GG
Exogenous TPX2	F : CGCACCATCTTCTTCAAGGA R : CAAATTGGCCTTCTCCTCAA
eGFP	F : CCG GAC CTC CAA AGA AAA A R : AAA AGT GAC CCC CGA CCT T
BCL2L1	F : GAT CCC CAT GGC AGC AGT AAA GCA AG R : CCC CAT CCC GGA AGA GTT CAT TCA CT
BIRC5	F: GGA CCA CCG CAT CTC TAC R: GCA CTT TCT TCG CAG TTT
YAP	F: GTG AGC CTG TTT GGA TGA TG R: CAC TGG ACA AAG GAA GCT GA
TAZ	F : CCA GGT GCT GGA AAA AGA AG R : CAG GAT GAT GGG GTT GAG AT
CTGF	F : CCA ATG ACA ACG CCT CCT G R : TGG TGC AGC CAG AAA GCT C
SERPINE1	F: TTG AAT CCC ATA GCT GCT TGA AT R: ACC GCA ACG TGG TTT TCT CA
SMAD4	F: GTC TGG CTT AAG GAG AGC CAT ACT R: GATACCTGCAACTCACCTTCCTAC

Table 2. siRNA sequence

Gene Symbol	siRNA sequence (5’ to 3’)
TPX2	S : CAG GAU UUU GCU GUG AAG U AS : ACU UCA CAG CAA AAU CCU G
AXL	S : GAC UGU CUG GAU GGA CUG U AS : ACA GUC CAU CCA GAC AGU C
TEAD4	S : CCG CCA AAU CUA UGA CAA ATT AS : UUU GUC AUA GAU UUG GCG GTT
YAP	S : CAG AAG AUC AAA GCU ACU U AS : AAG UAG CUU UGA UCU UCU G
TAZ	S : ACG UUG ACU UAG GAA CUU U AS : AAA GTT CCT AAG TCA ACG T

Results

1. Isogenic pair model H9-P1, P4

First of all, To investigate whether long-term propagation has effects on chromosomal integrity of cultured hESCs, we established the four variants of H9 hESC lines with various passage numbers (P1: 40s, P2: 100s, P3: 200s, and P4: 300s). This well-defined isogenic pair model is also used in paper published[36]. P4, the latest passage shows various genetic alteration including T12 (Fig.6A), but each isogenic pair has pluripotency, as proved with mRNA level and endogenous protein level of OCT4, SOX2 (Fig. 6B, 6C), and surface marker SSEA4, Nanog, and OCT4 staining (Fig.6D). It has been well known that genetic alteration might affects in lineage specification during differentiation[37], but this result indicates T12 and gain of 20q11.21 does not defect pluripotency of hESCs itself.

Although with T12, genetic alteration clearly shown in long-term cultured H9 (P3, P4) especially CNV in 20q11.21 locus. CNV including 20q11.21 loci occurs even in the early passage(Fig.7A) As previously known, almost 25% of hESCs have altered copy number variation(CNV), even if their karyotype

is normal[38]. Besides, driver events should be initiated in early passage to provoke passenger mutations including loss or gain of chromosome[14]. According to points listed above, cell model for studying driver of mutation should include not only isogenic pair for early and late passaged cell, but also cells in intermediate course that shows accumulation of mutation. This isogenic pair is appropriate for purpose that clearly shows CNVs accumulating during culture as shown in Fig. 7B. *BCL2L1*, the gene codes well-known anti apoptotic protein BCL-xL, is clearly induced not only in mRNA level but also in protein level, indicates clear survival advantage occurs in hESCs over 200 passages (Fig. 7C, 7D). In addition, the fact that not all genes located at 20q11.21 are gained narrows down the candidate for driver of genetic alteration (Fig. 7E). Of note, these clones showed the identical short tandem repeat profiles compared to control H9 hESCs(WiCell), implying they were derived from the same genetic background of an embryo(Fig.7F). Only difference in this isogenic pair is number of maintenance.

As expected, long term cultured hESCs over 200 passages (P3 and P4 hESCs) showed the aberrant chromosome segregation during mitosis (Fig. 8A), high incidences of chromatin bridge (Fig. 8B). As consistent with the previous studies that excessive numbers of centrosomes were closely linked to the improper chromosome segregation[39], supernumerary centrosomes were

more frequently observed in P4 compared to P1(Fig. 8C). This passage dependent increasement of lagging chromosome shows stepwise accumulation of genetic alteration. P4 shows more lagging chromosome compared to P1, and even to P3. Hence, P4 revealed the significant retardation of mitotic progression, more significantly different from P1 than P3 (Fig. 8D). Even P3 shows aberrant mitosis including increasement of lagging chromosome and CNV in 20q11.21, P4 gets more highly aborted mitosis. All this result shows there are another event between P3 and P4, indicating stepwise mutation-selection model for progression.

With all results reflecting accumulation of mutations, this isogenic cell model shows clear biological consequence of hESCs after long-term in vitro culture is the growth advantage[21][40], as co-cultured P4 with eGFP tagged P1 became dominant after 9weeks of culture. Together, P4 has resistance to mitotic stress induced by nocodazole treatment(Fig. 9B, 9C) or DNA damage[41] caused by YM155(Fig. 9D). Importantly, the most clear phenotype of the genetic aberration of hPSCs is ‘survival advantage’, which is referred as ‘culture adaptation’ [14], our model is obviously shows features for imitating culture adaptation. Fact that culture adapted P4 has resistance to aberrant mitosis is consistent with thesis about role of survival from mitotic stress is associated to gaining aneuploidy, as resent study also

demonstrating [35] [26]. Thus, survival advantage acquired by ‘culture adaptation’ in hPSCs, which leads not only to the resistance to cell death but also but also escape from the mitotic death would be relevant to increase of polyploidy of LP-hESCs.

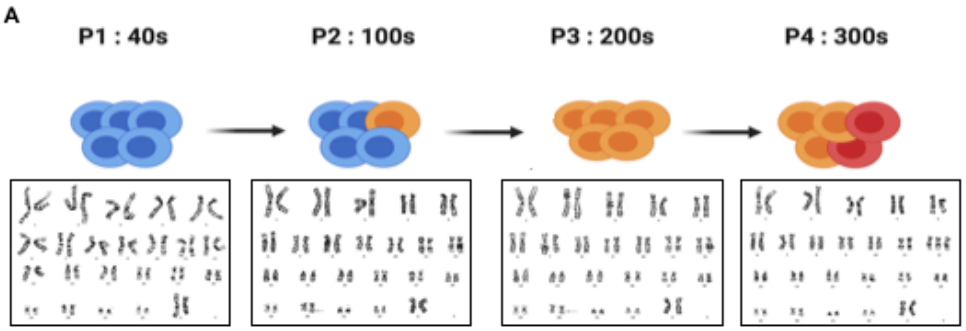
A
P1 : 40s
P2 : 100s
P3 : 200s
P4 : 300s

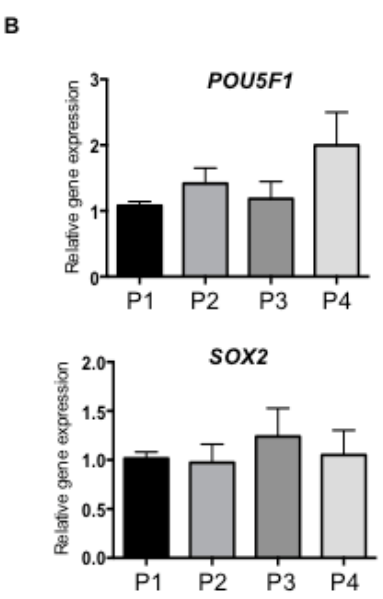
B
POU5F1
Relative gene expression
0
1
2
3
P1
P2
P3
P4
SOX2
Relative gene expression
0.0
0.5
1.0
1.5
2.0
P1
P2
P3
P4

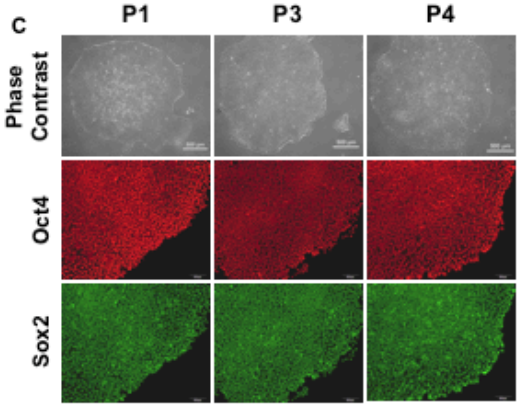
C
P1
P3
P4
Phase Contrast
Oct4
Sox2

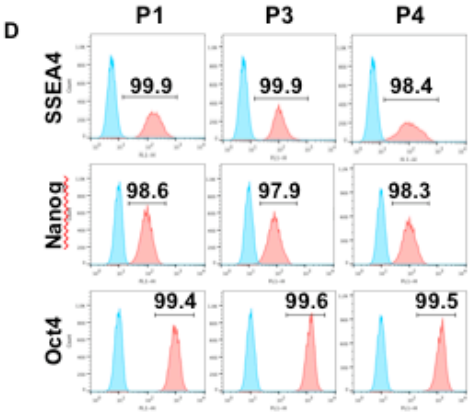
D
P1
P3
P4
SSEA4
99.9
99.9
98.4
Nanog
98.6
97.9
98.3
Oct4
99.4
99.6
99.5

Figure 6. Isogenic pair model P1, P4

(a) Isogenic pair model of H9 hESC with various passage numbers (P1: 40s, P2: 100s, P3: 200s, and P4: 300s) is used in this study. G-banded karyotyping was used to detect aneuploidy. **(b)**The latest passaged P4 shows various genetic alteration including T12 without loss of pluripotency. mRNA level of pluripotency marker POU5F1, SOX2 in P4 is not separated from P1. **(c)** Pluripotency marker Oct4, Sox2 is undifferentiated in protein level, tested by immunofluorescence. **(d)** Surface marker of pluripotency is unchanged in P4 compared to P1.

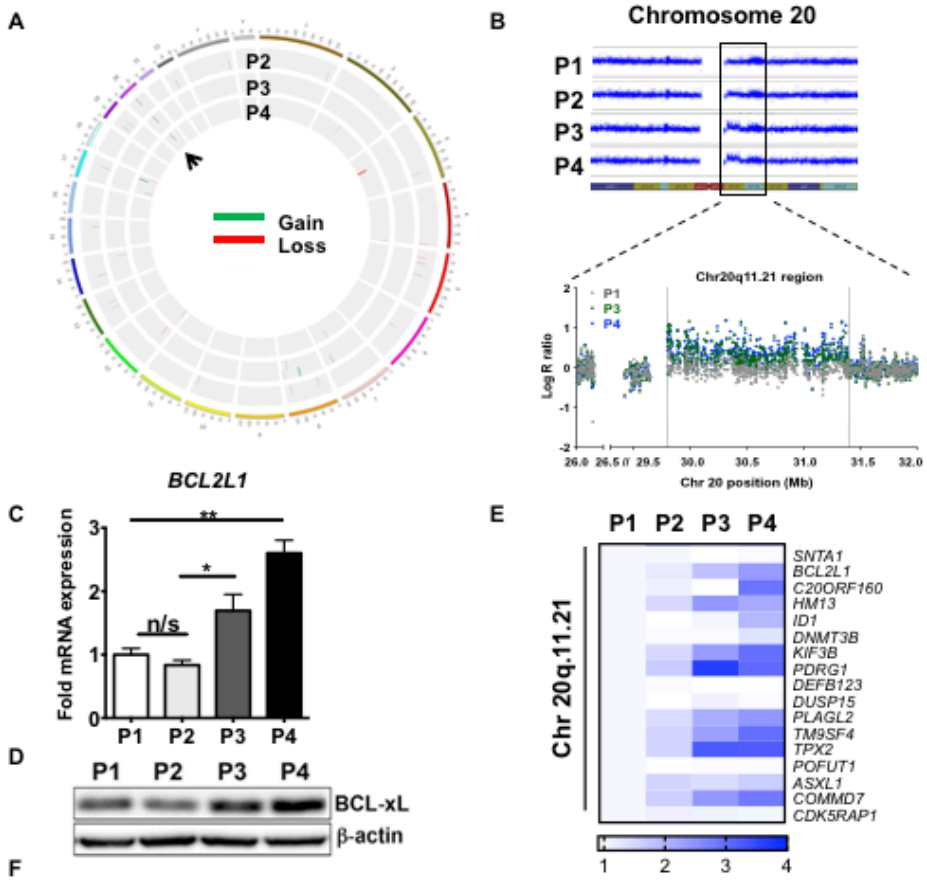

Samples	D16S539	D7S820	D13S317	D5S818	CSF1PO	TPOX	Amelogenin	TH01	vWA
H9 (WiCell)	**12, 13**	**9, 11**	**9, 9**	**11, 12**	**11, 11**	**10, 11**	**X, X**	**9.3, 9.3**	**17, 17**
P1 (40s)	**12, 13**	**9, 11**	**9, 9**	**11, 12**	**11, 11**	**10, 11**	**X, X**	**9.3, 9.3**	**17, 17**
P3 (200s)	**12, 13**	**9, 11**	**9, 9**	**11, 12**	**11, 11**	**10, 11**	**X, X**	**9.3, 9.3**	**17, 17**
P4 (300s)	**12, 13**	**9, 11**	**9, 9**	**11, 12**	**11, 11**	**10, 11**	**X, X**	**9.3, 9.3**	**17, 17**

Figure 7. Genetic alteration of P4

(a) CIRCOS plot for gain or loss of CNVs detected by SNP array, Human 22 and XY chromosomes were represented as the outer track with each tick indicating 5 Mbps. Each circle from the outer to inner track represents the copy-number profile of the P2, P3, and P4, respectively (green for the regions with gain and red for the regions with loss. **(b)** The detected CNVs ranged in size were quantified in P2, P3, P4. **(c-d)** reference from Cho et al., Stem Cell Reports(2018) **(c)** mRNA expression of BCL2L1 gradually increased during passage. One-way ANOVA, n=2, p=0.0376 for P3, p=0.0018 for P4 compared to P1. **(d)** Induction of BCL2L1 increased not only in mRNA but also in protein level. **(e)** Frequency of CNVs depending on size detected in LP-hESCs. Genomic profiles of P1 was used as a reference genome. **(f)** P1, P2, P3, P4 clones showed the identical short tandem repeat profiles compared to control H9 hESCs (WiCell), implying they were derived from the same genetic background of an embryo.

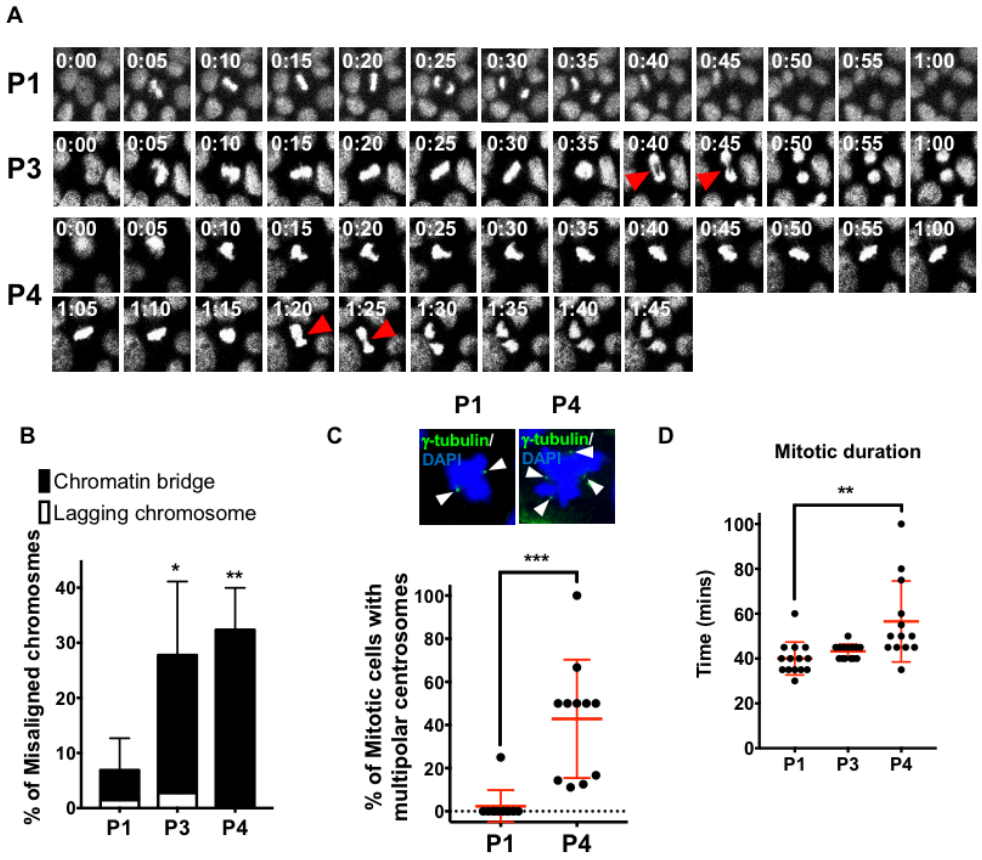
A
P1
P3
P4
0:00
0:05
0:10
0:15
0:20
0:25
0:30
0:35
0:40
0:45
0:50
0:55
1:00
1:05
1:10
1:15
1:20
1:25
1:30
1:35
1:40
1:45
B
Chromatin bridge
Lagging chromosome
% of Misaligned chromosmes
*
**
P1
P3
P4
C
P1
P4
γ-tubulin/
DAPI
***
% of Mitotic cells with multipolar centrosomes
P1
P4
D
Mitotic duration
**
Time (mins)
P1
P3
P4

Figure 8. P4 with aberrant mitosis

(a) Time-lapse images of chromosome alignment, scale bar = 10μm, Cells were stained with DAPI after release from nocodazole-induced prometaphase until indicative time points(P1: 40s, P3: 200s, and P4: 300s). Two-Way ANOVA. N=3, p=0.0131 for P2, p=0.0013 for P4 compared to P1. **(b)** Cells with cytokinetic failure were counted after time-laps imaging. **(c)** Cells were stained with γ-tubulin (red) or TPX2 (green) to visualize centrosomes (arrowhead, scale bar = 10μm). Percentages of mitotic cells showing multi-centrosomes were represented as a scatter plot. Unpaired t-test, n = 11, ***p = 0.0003. **(d)** Mitotic duration of cells were counted after time-laps imaging. One-Way ANOVA, n=14, p=0.0009 for P4 compared to P1.

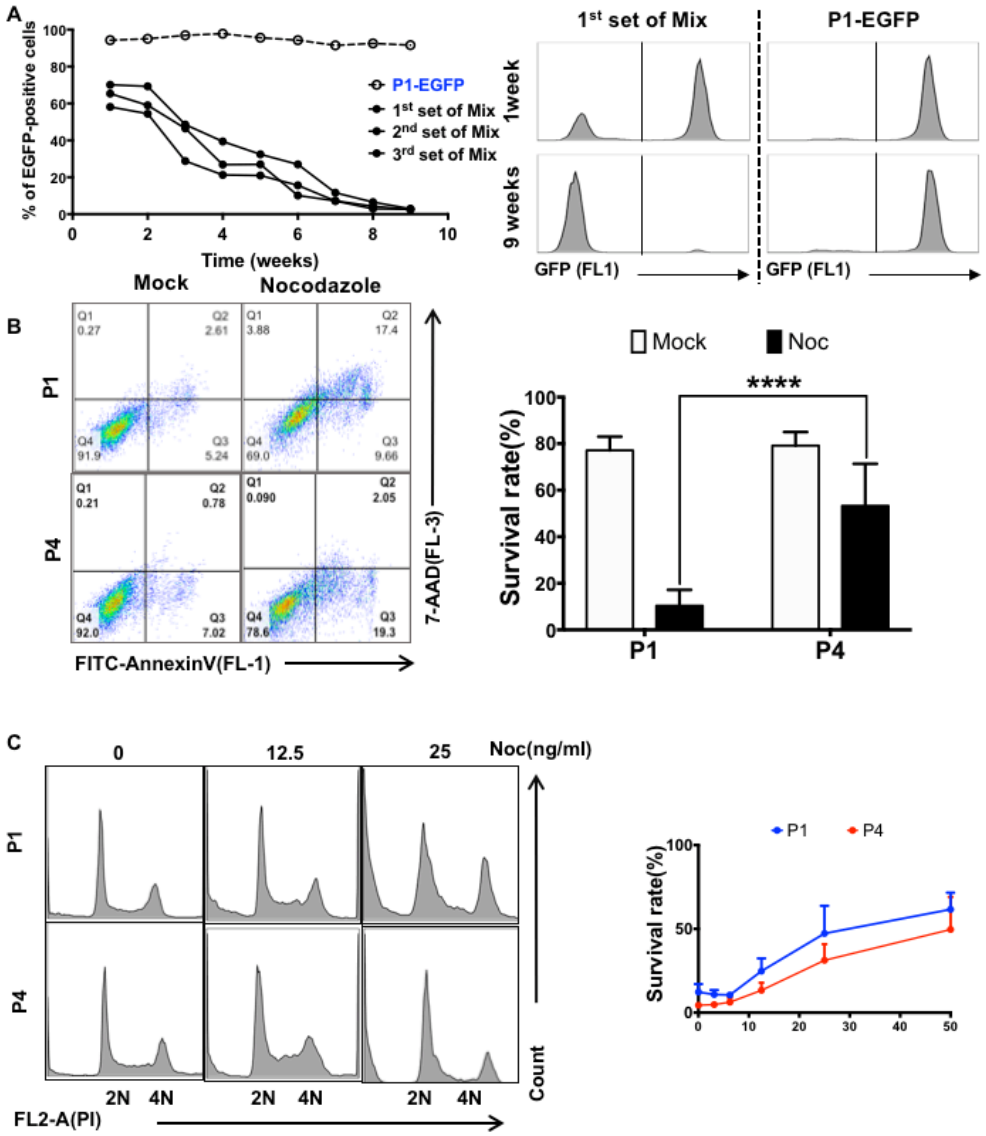
A
% of EGFP-positive cells
Time (weeks)
P1-EGFP
1st set of Mix
2nd set of Mix
3rd set of Mix
1st set of Mix
P1-EGFP
1week
9 weeks
GFP (FL1)
GFP (FL1)
B
Mock
Nocodazole
P1
P4
7-AAD(FL-3)
FITC-AnnexinV(FL-1)
Mock
Noc
****
Survival rate(%)
P1
P4
C
0
12.5
25
Noc(ng/ml)
P1
P4
2N 4N
2N 4N
2N 4N
Count
FL2-A(PI)
P1
P4
Survival rate(%)

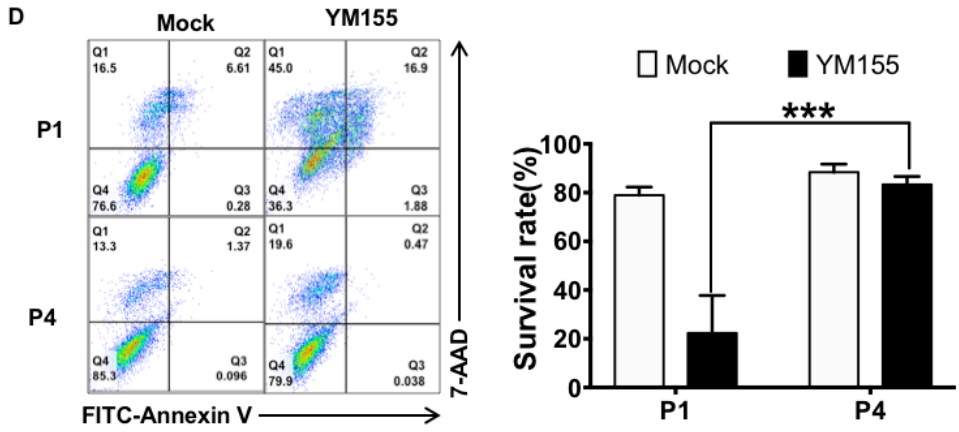

Figure 9. High Resistance of P4 to cell death stimuli

(a) Co-cultured P1-eGFP and P4. P4 clearly overwhelmed P1 after long term culture. Right panel shows FACS result.**(b)**Cell death in P1 and P4 under Nocodazole 50ng/ml was tested in FACS analysis, stained by Annexin V and 7-AAD. (Two-way ANOVA, n=5, $p<0.0001$). **(c)** Cell cycle differentiation in P1 and P4 under nocodazole stress was tested by PI staining. Right panel shows survival rate, calculated by SubG1 population.**(d)** P1 and P4 under DNA damage caused by 50μM of YM155. After treatment, cell death detected by AnnexinV/7-AAD staining was measured. (P1 and P4 under DNA damage caused by 50 μ M of YM155. After treatment, cell death detected by AnnexinV/7-AAD staining was measured. (two-way ANOVA. n=6, p = 0.0004.)

2. TPX2 as a candidate driver

Among the genes contained in 20q11.21 locus (Fig. 10A), we attempted to identify a gene responsible for survival during aberrant mitosis in LP-hESCs. First of all, to narrow down a candidate, mRNA level was measured(Fig. 10B). Including well-known survival regulator BCL2L1[21], TPX2, KIF3B, and NANOG regulator ID1[42] were significantly increased in P4, and also in P3. To achieve the comprehensive functional annotations of genes commonly amplified in CNVs and mRNA, we performed the gene ontology (GO) analysis using the web-based tool ConsensusPathDB (http://cpdb.molgen.mpg.de/). Interestingly, among genes in 20q11.21 locus, TPX2 and KIF3B genes were consistently included in both GO terms ('Spindle organization' and 'Cytoskeleton organization') as shown in Fig. 10C. Notably, TPX2 showed the top 'core enrichment' in GSEA plots for 'Microtubule based process' and 'Microtubule polymerization or de-polymerization' among the genes of 20q11.21 locus as shown in Figure 10D. Two genes, TPX2 and KIF3B are both responsible for microtubule regulation, and also up-regulated in culture adapted P4 (Fig. 10F). More importantly, TPX2, which has diverse roles in microtubule nucleation and spindle assembly[43], and also known to have the highest 'CIN' score in multiple

cancer[33], we hypothesized that upregulation of TPX2 in LP-hESCs would be accountable for chromosomal abnormality resulting from perturbed microtubule dynamics.

To determine the genomic levels of TPX2 in P4, SNP array was done. As predicted, TPX2 showed clear induction in P4 compared to P1 in DNA (Fig.11A), mRNA (Fig.11B), and protein(Fig.11C) level. Passage dependent expression was determined by the dual staining of TPX2 and DNA content with 7-AAD (Fig. 11D). Intriguingly, TPX2 level of protein and mRNA are increasing until P3 but declined in P4, indicates there are other differentiation event between two late passaged hESCs. Given that TPX2 protein, regulated in cell cycle dependent manner, is highly upregulated at G2/M phase[44], the high TPX2-positive population in P3 and P4 would not result from more G2/M population of P3 and P4 hESCs due to similar cell cycle profile compared to P1 (Fig. 11E).

Meanwhile, Aurora kinase A, a microtubule dynamics regulator[45], and also critical for maintenance of pluripotency of ESCs by suppression of p53[46], shows high phosphorylation in P4(Fig. 12A). It is noteworthy that TPX2 serves as a positive regulator of Aurora A kinase, encoded by AURKA [47]. Accordingly, active phosphorylation of Aurora A was manifested in P3 and P4 hESCs along with high TPX2 expression. Aurora kinase A also predicted

as selective killer of culture adapted P4, by using bioinformatic analysis (Fig. 12B). First of all, DEG from RNA-seq result was prepared. Next, cancer cell line which expresses similar DEG (Differently Expressed Genes) with P1 and P4 was selected based on CCLE (Cancer Cell Line Encyclopedia) to discover set of compounds with selective toxicity by drug sensitivity database CTRP(https://portals.broadinstitute.org/ctrp/). This prediction based on DEG, CCLE and CTRP are proved to be efficient in other paper[36]. The result that AURKA inhibitor predicted as selective killer of P4 while other DNA damaging agent YM155 or mitotic damage inducer nocodazole does not, gives insight for importance of AURKA in culture adaptation and survival advantage in P4. As conclusion, TPX2-AURKA axis is predicted to be important in culture adaptation in P4, while mechanism of advantage is not yet defined.

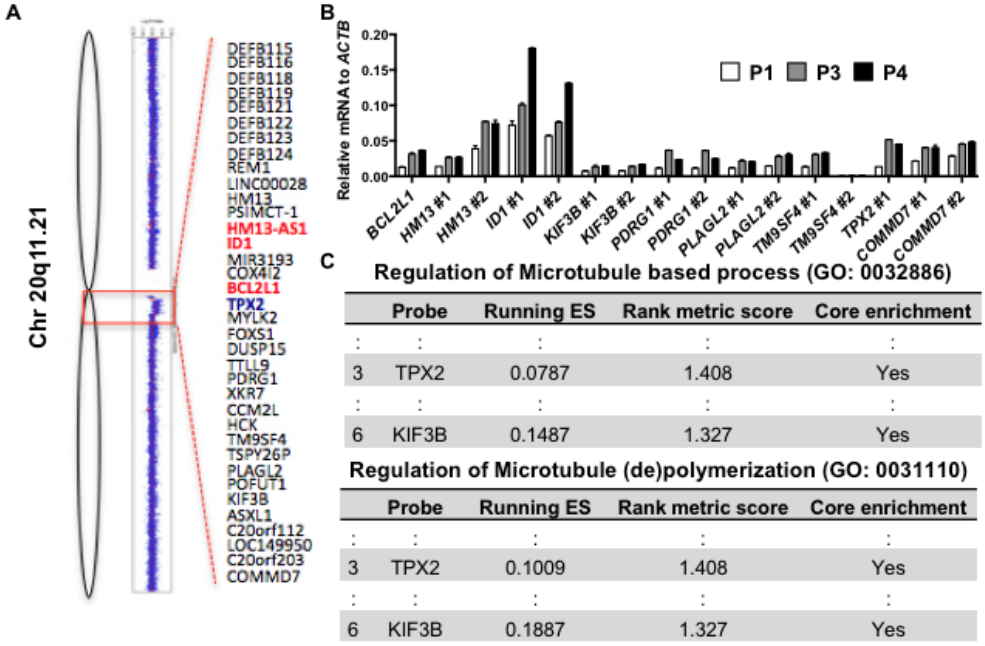

C

Regulation of Microtubule based process (GO: 0032886)

	Probe	Running ES	Rank metric score	Core enrichment
:	:	:	:	:
3	TPX2	0.0787	1.408	Yes
:	:	:	:	:
6	KIF3B	0.1487	1.327	Yes

Regulation of Microtubule (de)polymerization (GO: 0031110)

	Probe	Running ES	Rank metric score	Core enrichment
:	:	:	:	:
3	TPX2	0.1009	1.408	Yes
:	:	:	:	:
6	KIF3B	0.1887	1.327	Yes

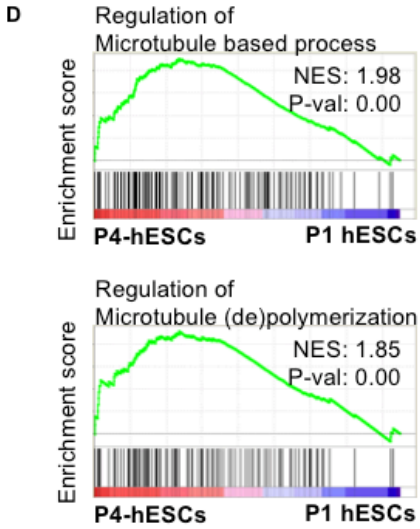

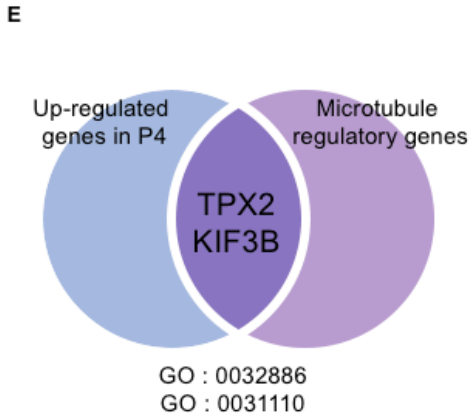

Figure 10. TPX2 as a candidate driver

(a) Lists for genes in 20q11.21 locus. **(b)**mRNA level was measured for genes in 20q11.21 locus, **(c)**Gene ontology (GO) analysis using the web-based tool ConsensusPathDB was shown. Only two gene related were shown. **(d)** GSEA assay based on RNA-seq data. P4 shows increasement in gene sets related to regulation of microtubule based process, and regulation of microtubule depolymerization. **(e)** Summary of gene analysis. TPX2 and KIF3B are only genes both enriched in P4, and regulating microtubule.

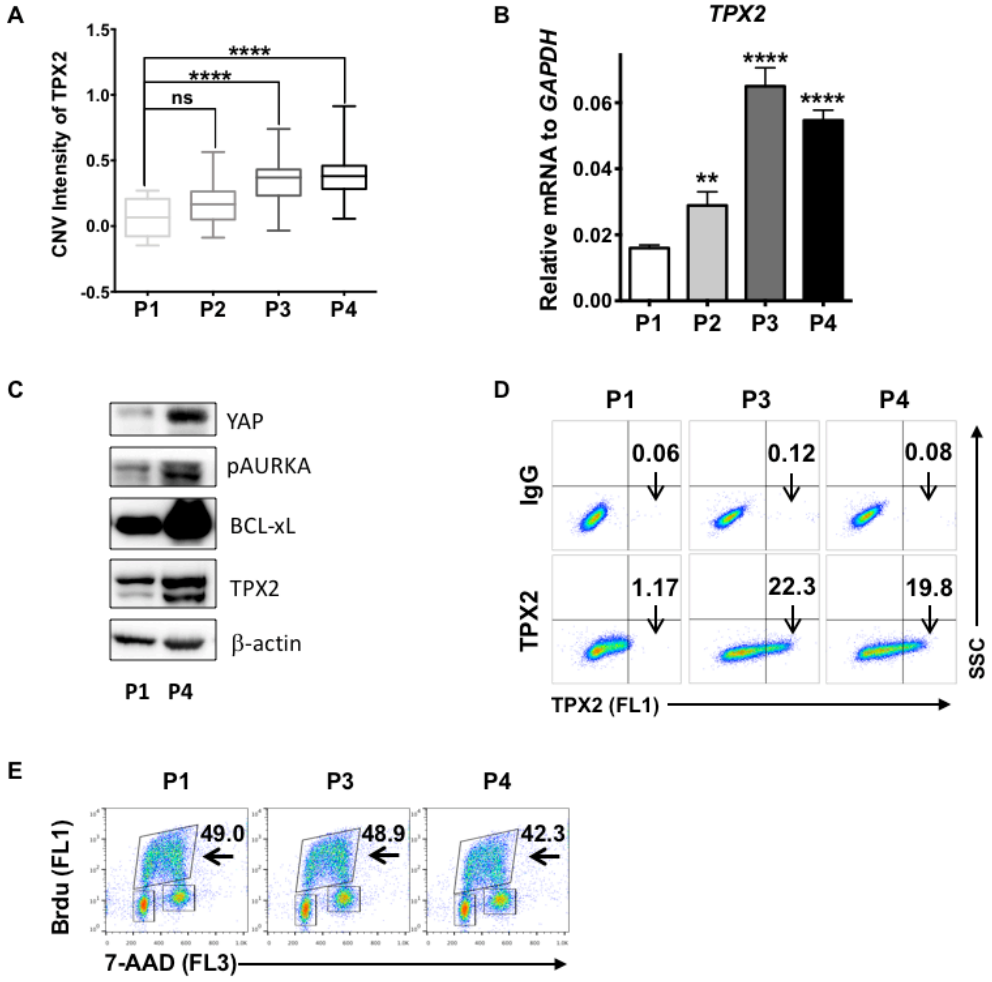
A
CNV Intensity of TPX2
1.5
1.0
0.5
0.0
-0.5
****
****
ns
P1
P2
P3
P4
B
TPX2
Relative mRNA to GAPDH
0.06
0.04
0.02
0.00
**
****
****
P1
P2
P3
P4
C
YAP
pAURKA
BCL-xL
TPX2
β-actin
P1 P4
D
P1
P3
P4
IgG
TPX2
0.06
0.12
0.08
1.17
22.3
19.8
SSC
TPX2 (FL1)
E
P1
P3
P4
Brdu (FL1)
49.0
48.9
42.3
7-AAD (FL3)

Figure 11. High TPX2 level in P4

(a) Intensity shows increased CNV in P4 compared to P1. One-Way ANOVA, n=14. $p < 0.0001$ for both P3 and P4. **(b)** mRNA level of TPX2 is significantly high in late passaged cells. One-Way ANOVA, n=4, $p=0.0023$ for P2, $p<0.0001$ for P3 and P4, compared to P1. **(c)** Protein level of TPX2, BCL-xL is up-regulated in P4, with activated Aurora Kinase A. **(d)** Protein expression level of TPX2 was tested by immunostaining. More population with induced TPX2 was discovered in P3 and P4. **(e)** Cell cycle was tested by Brdu staining, and there was no difference in length of G2/M. This indicates that increased protein level in P4 is not because of cell cycle alteration.

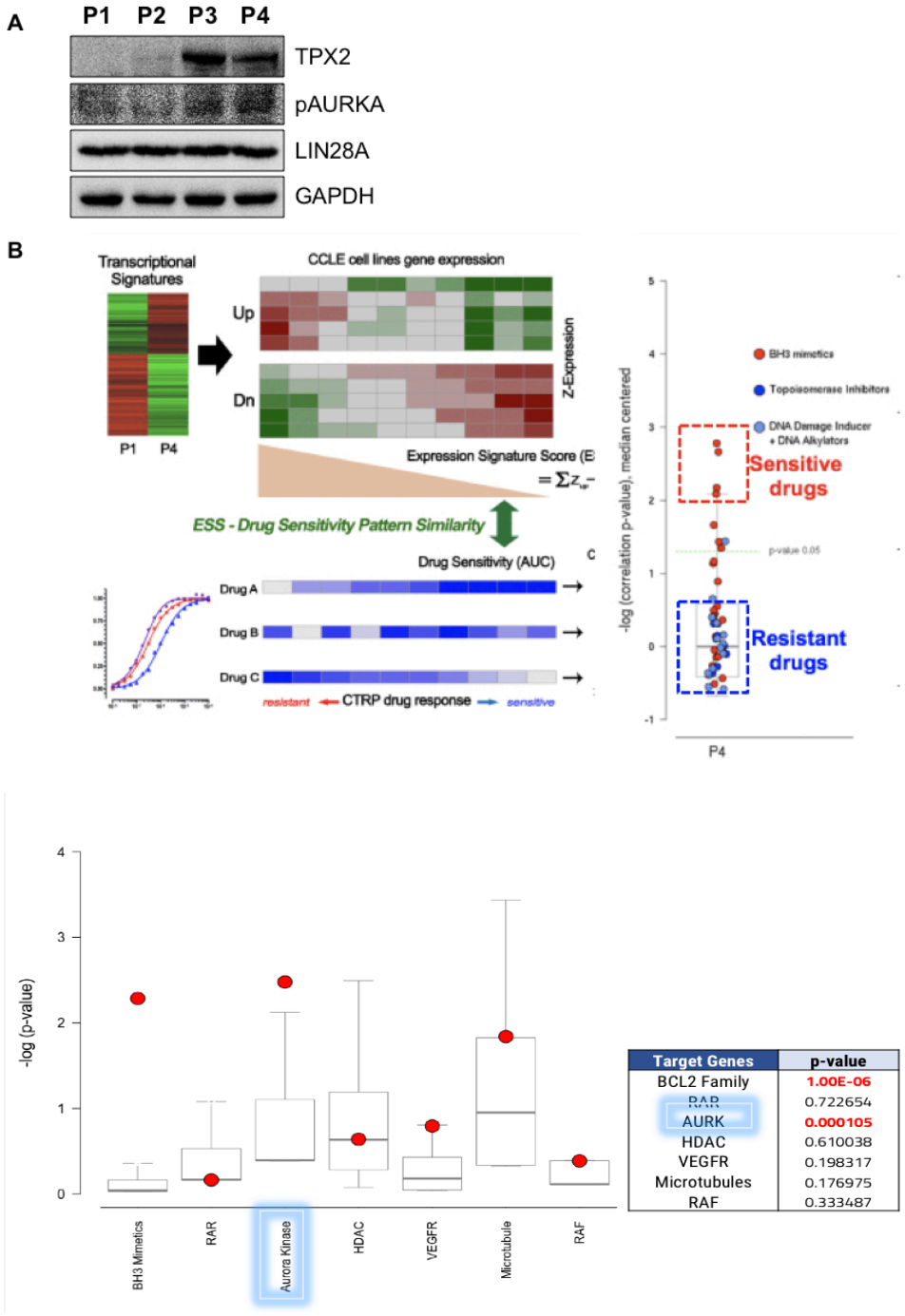
A
P1
P2
P3
P4
TPX2
pAURKA
LIN28A
GAPDH
B
Transcriptional Signatures
P1
P4
CCLE cell lines gene expression
Up
Dn
Z-Expression
Expression Signature Score (E
= Σz_i
ESS - Drug Sensitivity Pattern Similarity
Drug Sensitivity (AUC)
Drug A
Drug B
Drug C
resistant
CTRP drug response
sensitive
-log (correlation p-value), median centered
BH3 mimetics
Topoisomerase Inhibitors
DNA Damage Inducer + DNA Alkylators
Sensitive drugs
p-value 0.05
Resistant drugs
P4
-log (p-value)
BH3 Mimetics
RAR
Aurora Kinase
HDAC
VEGFR
Microtubule
RAF
Target Genes
p-value
BCL2 Family
1.00E-06
RAR
0.722654
AURK
0.000105
HDAC
0.610038
VEGFR
0.198317
Microtubules
0.176975
RAF
0.333487

Figure 12. High dependency of Aurora A kinase for survival

(a) Active phosphorylation of Aurora Kinase A gradually increased in late passaged hESCs. **(b)** Prediction of selective killer of culture adapted hESCs based on DEG (Differently Expressed Genes) based on RNA-seq data. Cancer cell line which expresses similar DEG with P1 and P4 was selected based on CCLE (Cancer Cell Line Encyclopedia). CTRP predicted set of compounds with selective toxicity. This result shows TPX2/AURKA axis serves important role in culture adapted hESCs.

3. Establishment of Dox inducible TPX2 model

To examine effect of TPX2 in mitotic survival, hESC-H9 cell line with inducible overexpression TPX2 was established. Protein of interest was tagged by eGFP to make it easy to trace expression, localization, and function of exogenous TPX2. While hESCs with stably expressing TPX2 failed to maintain in unknow reason, conditionally expressed TPX2 successfully increased in Doxycycline dose dependent manner (Fig. 13B), as eGFP increases with TPX2(Fig.13C). To rid out copy number variation of transfected TPX2, single clone population was selected after picking based on protein, mRNA level and function of TPX2. H9-iTPX2-#4 shows clear enrichment of endo- and exogenous TPX2 protein than pool population (Fig. 13D). H9-iTPX2-#5 also shows increased TPX2 with eGFP, as constant with pool and single colony #4(Fig. 13E). TPX2 tagged with eGFP clearly localizes to microtubule during mitosis (Fig.13F). TPX2 overexpression does not alter pluripotency of hESCs, as shown in Fig.14A, but excess level of exogenous TPX2 cause cell growth arrest(Fig.14B), and cell cycle arrest in G2/M(Fig. 14C). It would account for the repeated failure of establishment of TPX2 stable hESCs with slight leakage of inducible vector(Fig.14D).

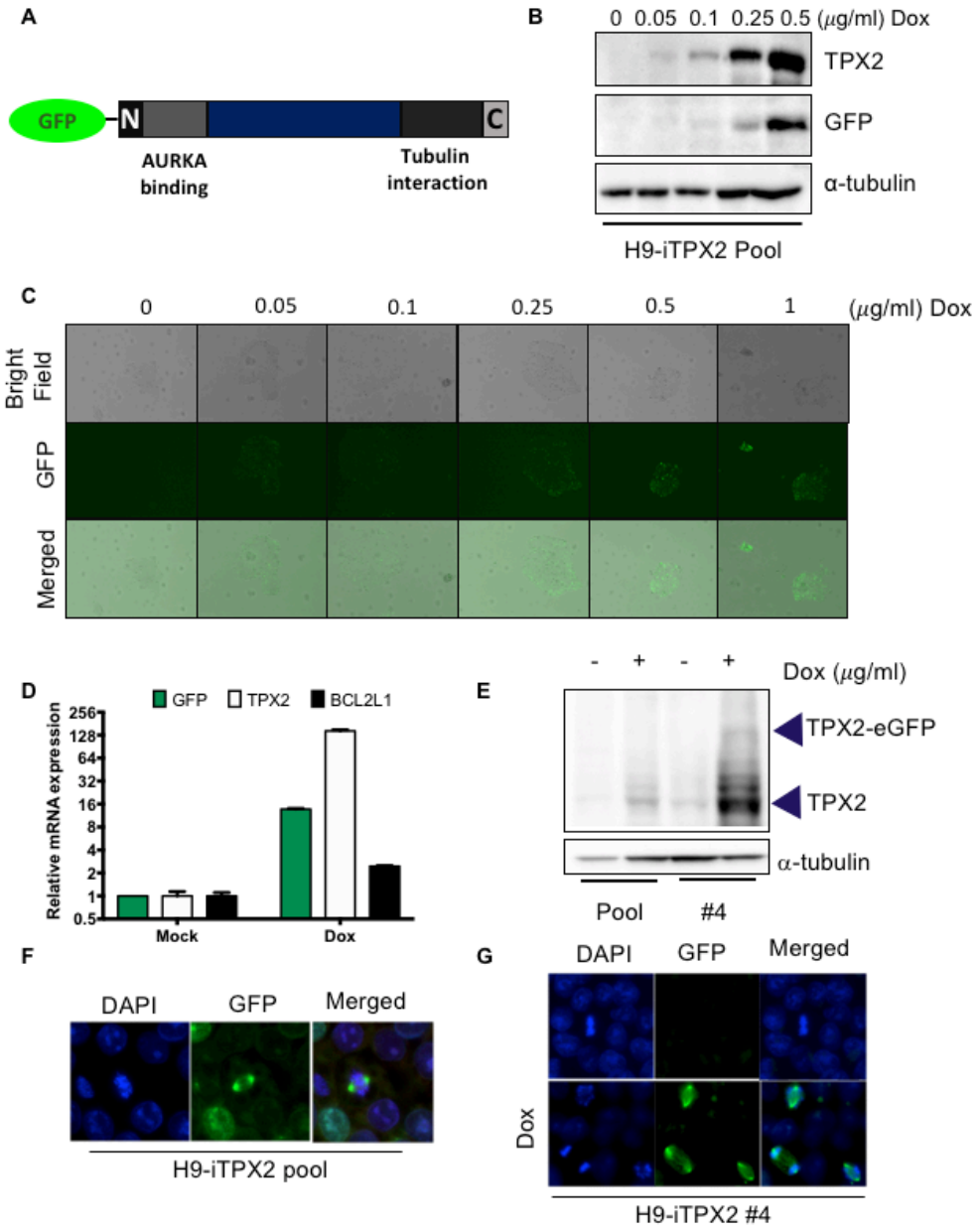
A
GFP
N
C
AURKA binding
Tubulin interaction
B
0 0.05 0.1 0.25 0.5 (μg/ml) Dox
TPX2
GFP
α-tubulin
H9-iTPX2 Pool
C
0
0.05
0.1
0.25
0.5
1
(μg/ml) Dox
Bright Field
GFP
Merged
D
GFP
TPX2
BCL2L1
Relative mRNA expression
256
128
64
32
16
8
4
2
1
0.5
Mock
Dox
E
- + - +
Dox (μg/ml)
TPX2-eGFP
TPX2
α-tubulin
Pool
#4
F
DAPI
GFP
Merged
H9-iTPX2 pool
G
DAPI
GFP
Merged
Dox
H9-iTPX2 #4

Figure 13. Establishment of Dox inducible TPX2 model

(a) Scheme of inducible overexpression TPX2 tagged with eGFP. **(b)** TPX2 and GFP expression in inducible cell line was examined, showed system working. Doxycycline was treated for 24hr before assay. IB shows increasement of TPX2 and GFP in protein level, as dox dose dependent manner. **(c)** GFP was detected by fluorescence microscope increased doxycycline dose dependent manner. Doxycycline was treated for 24hr before observation. **(d)** Single colony #5 shows increased TPX2 and eGFP expression under 0.1μg/ml of Doxycycline treatment for 24hr. **(e)** Endogenous TPX2(over 100kda, under 130kda)and eGFP tagged TPX2(Over 130kda) was detected by IB. Doxycycline 0.1μg/ml was treated before sampling. Single clone #4 shows clearly high TPX2 expression under same concentration of Dox. **(f)** Pool, and #4 expressing TPX2-eGFR with clear localization to microtubule during mitosis. **(g)** Induced TPX2 in single clone #4 also showed correct function.

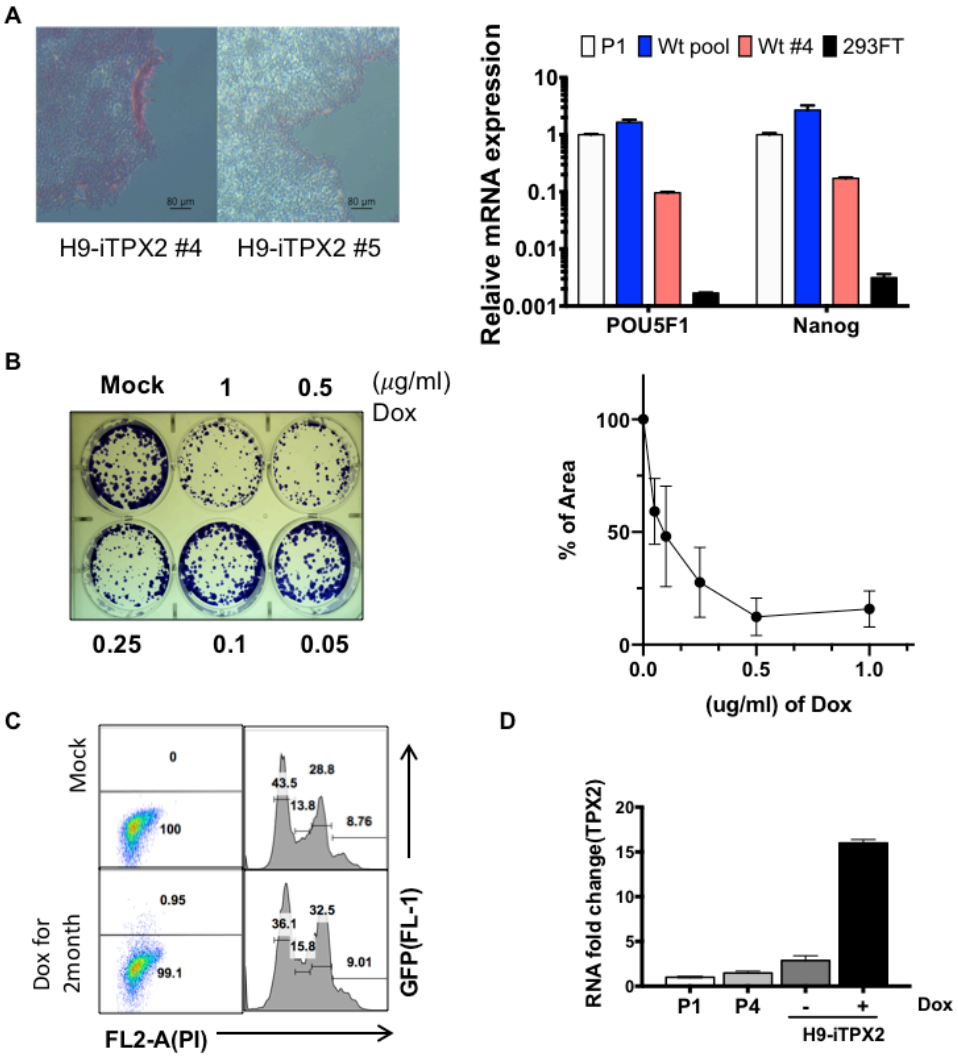
A
H9-iTPX2 #4
H9-iTPX2 #5
P1
Wt pool
Wt #4
293FT
Relaive mRNA expression
POU5F1
Nanog
B
Mock
1
0.5
(μg/ml)
Dox
0.25
0.1
0.05
% of Area
(ug/ml) of Dox
C
Mock
Dox for 2month
FL2-A(PI)
GFP(FL-1)
D
RNA fold change(TPX2)
P1
P4
Dox
H9-iTPX2

Figure 14. Effect of inducible TPX2 and Doxycycline treatment in H9

(a) Cells maintained from single colony #4 and #5 showed no difference in pluripotency. Left panel shows AP staining while right panel shows pluripotency marker expression. **(b)** Excess TPX2 expressed by high concentration of doxycycline cause cell cycle arrest, Left panel shows clonogenic assay result tested in H9-iTPX2 pool, and right panel displays quantification of area. Test was repeated twice. **(c)** PI staining shows continuously treated doxycycline cause G2/M arrest. **(d)** mRNA level of TPX2 was tested in P1, P4 and inducible TPX2 cell line. TPX2 was not only increased under doxycycline, but also without dox compared to P4.

4. TPX2 for survival under mitotic stress

TPX2 overexpressed cells were treated with nocodazole, to give mitotic stress. After low dose of doxycycline treatment for 24hr, High eGFP populations with exogenous TPX2, are more resistant to nocodazole, compared to endogenous control, eGFP null population of #4(Fig. 15A). This phenomenon repeated in lower concentration of nocodazole at #5, as shown in Fig. 15B. Intriguingly, damage induced by YM155, a DNA damaging agent, was not rescued by induction of TPX2, as shown in Fig.15C. Same was repeated in single clone #5(Fig.15D).

All this effect was repeated in other hESCs, CHA3. Inducible CHA3 cell line shows increased TPX2 and eGFP in protein level (Fig. 16A) and mRNA level (Fig.16B), with proper localization during mitosis (Fig.16C). TPX2 excess population as indicated with high eGFP are all resistant to mitotic stress induced by nocodazole compared to eGFP negative group(Fig. 16D), while damage of YM155 was not recovered in both population(Fig.16E). Consistent with results above, co-cultured H9-iTPX2#5 became dominant after nocodazole treatment under low dose of doxycycline (Fig.17B). H9-iTPX2#5 co cultured with eGFP tagged P1 without doxycycline also won the competition under nocodazole stress (Fig.17D). This indicates rescuing effect

of excess TPX2 is only effected in aberrant mitosis, not against other stress as DNA damage.

While induced TPX2 rescues cells from mitotic catastrophe, removal of TPX2 diminish survival advantage against mitotic stress in culture adapted hESCs, P4. Transient knockdown of TPX2 using siRNA results in significantly increased FITC-AnnexinV/7-AAD double positive group, as shown in Fig. 18A. Quantification and statics of survival rate differentiation is presented in Fig.18B. As indicated previously, lack of TPX2 is lethal in embryo level while heterogenic mutation is not[48]. Furthermore, cell with high efficiency of transfection and knockdown might be selected out during culture, results in low knockout efficacy (Fig. 18C). To clarify effect of TPX2, I tried knockout using CRISPR system. To avoid the low CRISPR-Cas9 activity in hPSCs[49], co-targeting YES approach was used[50](Fig. 18D). Guide RNA for eGFP and gene of interest are both transfected to CHA3-Cas9-eGFP, than followed by cell sorting by eGFP in order to select TPX2 hetero knockout cell. eGFP positive cell was regarded as internal control, while eGFP negative population including eGFP-TPX2 double KO cells is experimental group (Fig.18E). Despite of low proportion of double KO cell and sorting error, physiology of TPX2 KO is clearly seen under nocodazole treatment.

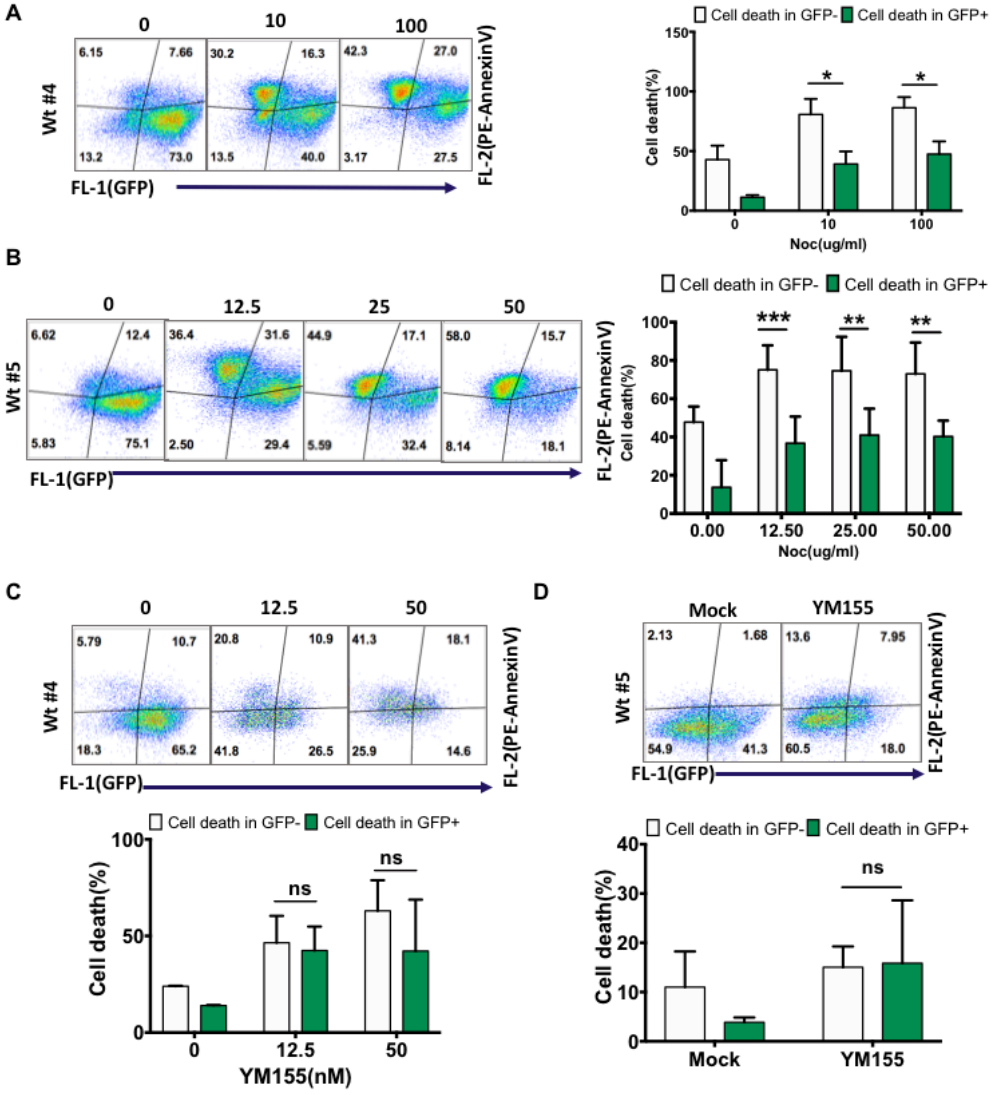
A
0
10
100
Wt #4
6.15
7.66
13.2
73.0
30.2
16.3
13.5
40.0
42.3
27.0
3.17
27.5
FL-1(GFP)
FL-2(PE-AnnexinV)
Cell death in GFP-
Cell death in GFP+
Cell death(%)
150
100
50
0
*
*
0
10
100
Noc(ug/ml)
B
0
12.5
25
50
Wt #5
6.62
12.4
5.83
75.1
36.4
31.6
2.50
29.4
44.9
17.1
5.59
32.4
58.0
15.7
8.14
18.1
FL-1(GFP)
FL-2(PE-AnnexinV)
Cell death in GFP-
Cell death in GFP+
Cell death(%)
100
80
60
40
20
0
***
**
**
0.00
12.50
25.00
50.00
Noc(ug/ml)
C
0
12.5
50
Wt #4
5.79
10.7
18.3
65.2
20.8
10.9
41.8
26.5
41.3
18.1
25.9
14.6
FL-1(GFP)
FL-2(PE-AnnexinV)
Cell death in GFP-
Cell death in GFP+
Cell death(%)
100
50
0
ns
ns
0
12.5
50
YM155(nM)
D
Mock
YM155
Wt #5
2.13
1.68
54.9
41.3
13.6
7.95
60.5
18.0
FL-1(GFP)
FL-2(PE-AnnexinV)
Cell death in GFP-
Cell death in GFP+
Cell death(%)
40
30
20
10
0
ns
Mock
YM155

Figure 15. TPX2 for survival under mitotic stress in H9

(a-b) TPX2 overexpression population can be distinguished from normal cells by level of eGFP. eGFP negative cells are used as internal control of cell death assay under nocodazole stress. eGFP-positive, TPX2 overexpressing cells showed clear survival advantage under nocodazole compared to internal control in two single clone. Unpaired t-test, nonparametric method was done. **(a)** #4 cell showed survival advantage under mitotic stress. n=4, p=0.0286 for 10μg/ml, and p=0.0286 for 100μg/ml. **(b)** #5 cell was tested in same method. n=8. p = 0.0002 for 12.5μg/ml, p= 0.0023 for 25μg/ml, and p=0.0012 for 50μg/ml of nocodazole. **(c-d)** Same assays were done by DNA damaging agent YM155. **(c)** For #4 clone, n= 4 and **(d)** n=7 for #5. This result shows induction of TPX2 gives survival advantage only under mitotic stress. All experiment is under 0.1μg/ml of doxycycline for 24hr pre-treatment. Media was exchanged to experimental condition with constant dose of doxycycline

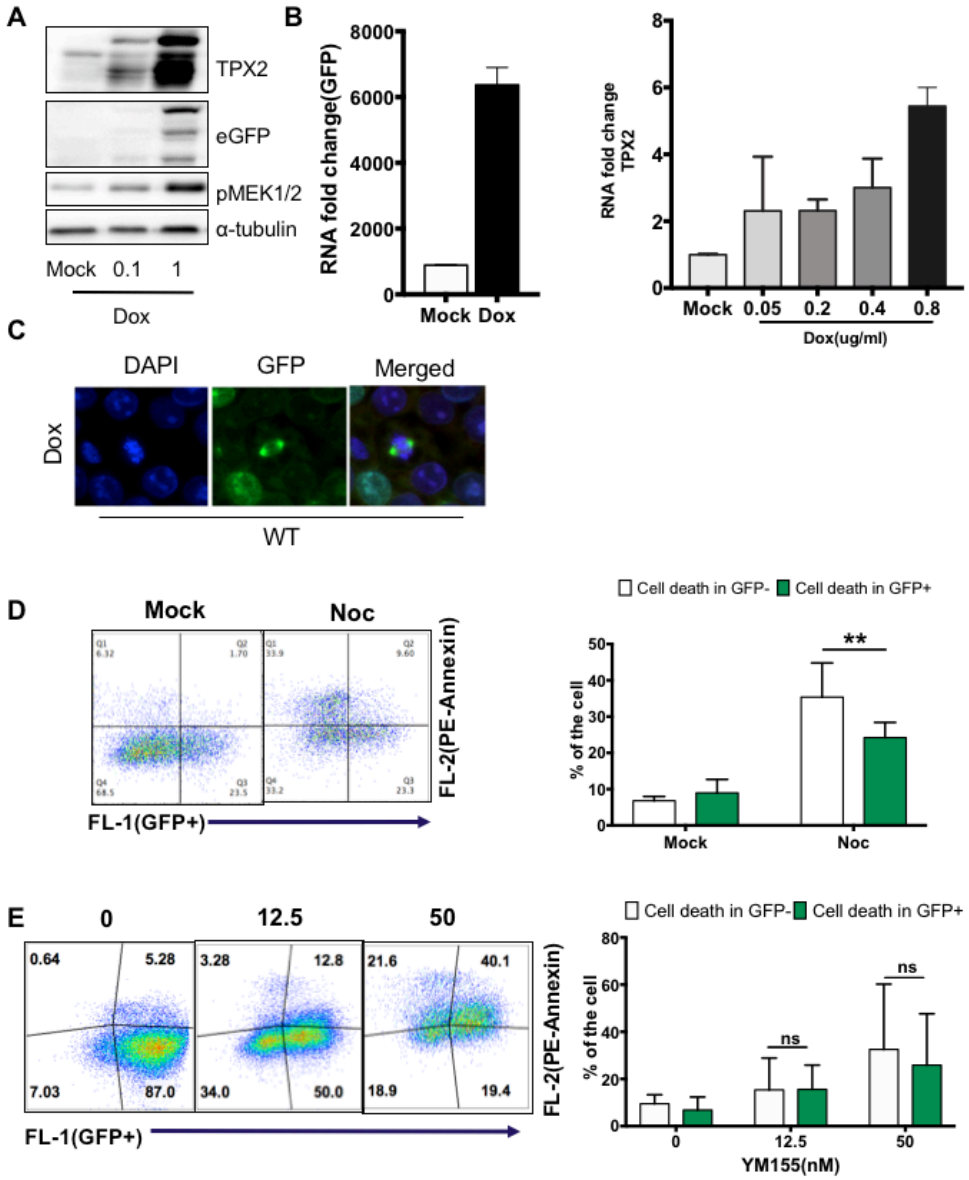
A
TPX2
eGFP
pMEK1/2
α-tubulin
Mock 0.1 1
Dox
B
RNA fold change(GFP)
8000
6000
4000
2000
0
Mock Dox
RNA fold change TPX2
8
6
4
2
0
Mock 0.05 0.2 0.4 0.8
Dox(ug/ml)
C
DAPI
GFP
Merged
Dox
WT
D
Mock
Noc
FL-2(PE-Annexin)
FL-1(GFP+)
Cell death in GFP-
Cell death in GFP+
% of the cell
50
40
30
20
10
0
**
Mock
Noc
E
0
12.5
50
0.64
5.28
7.03
87.0
3.28
12.8
34.0
50.0
21.6
40.1
18.9
19.4
FL-2(PE-Annexin)
FL-1(GFP+)
Cell death in GFP-
Cell death in GFP+
% of the cell
80
60
40
20
0
ns
ns
0
12.5
50
YM155(nM)

Figure 16. TPX2 for survival under mitotic stress in CHA3

(a) CHA3-iTPX2 shows increased expression of TPX2 and eGFP in dox dose dependent manner. **(b)** mRNA level of eGFP and TPX2 was also increased according to dox treatment. **(c)** Localization of TPX2 in mitotic spindle during mitosis is clearly seen by eGFP. **(d)** Rescuing effect of TPX2 under mitotic stress repeated in another cell, CHA3-iTPX2. n = 9, nonparametric unpaired t-test, p=0.0012. **(e)** Same experiment was done by YM155. TPX2 overexpression showed no difference in cell death rate under DNA damage. n=14, parametric unpaired t-test. All experiment without indication of doxycycline dose is under 0.1μg/ml of doxycycline for 24hr pre-treatment. Media was exchanged to experimental condition with constant dose of doxycycline.

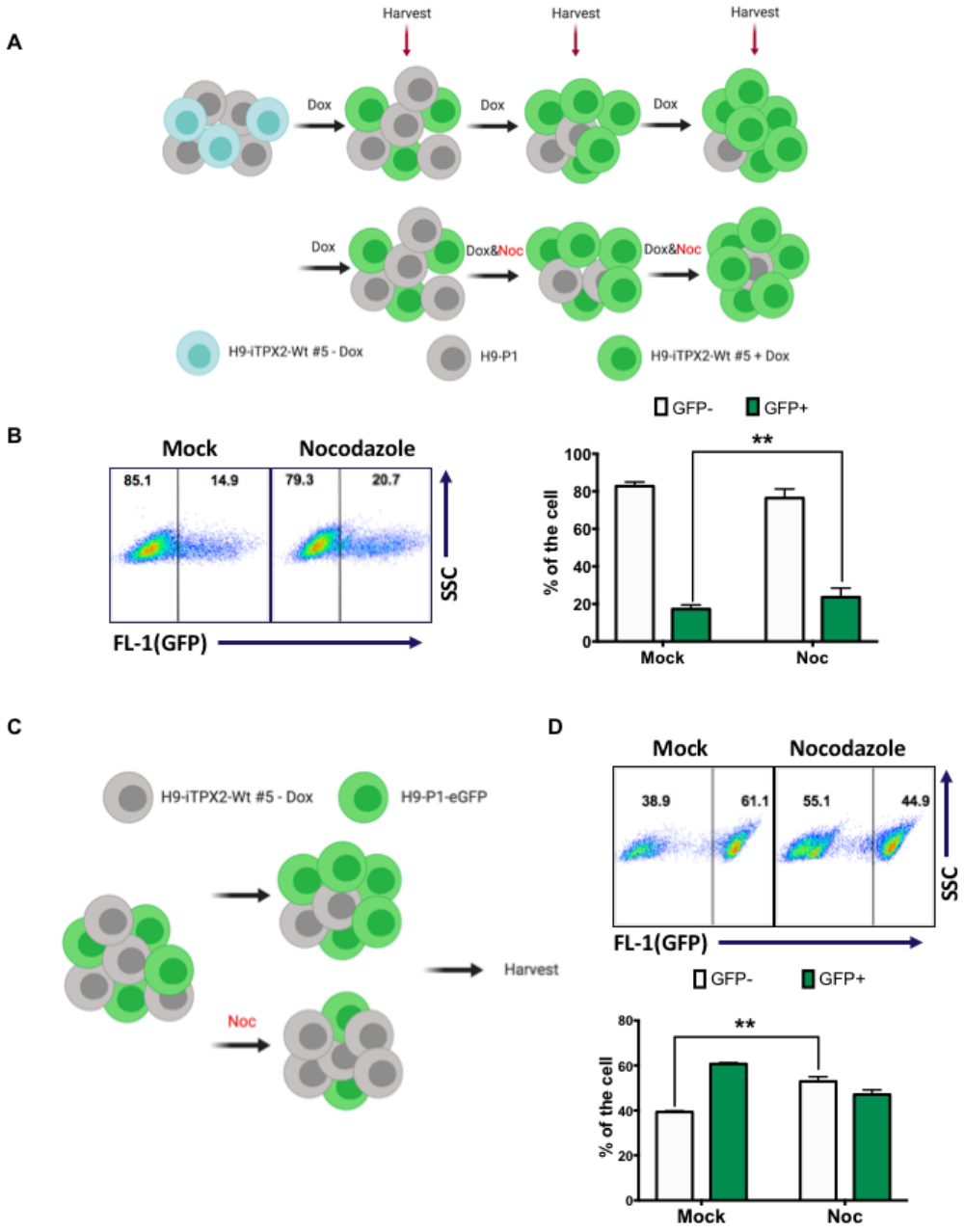
A
Harvest
Harvest
Harvest
Dox
Dox
Dox
Dox
Dox&Noc
Dox&Noc
H9-iTPX2-Wt #5 - Dox
H9-P1
H9-iTPX2-Wt #5 + Dox
B
Mock
Nocodazole
85.1
14.9
79.3
20.7
SSC
FL-1(GFP)
GFP-
GFP+
**
% of the cell
100
80
60
40
20
0
Mock
Noc
C
H9-iTPX2-Wt #5 - Dox
H9-P1-eGFP
Harvest
Noc
D
Mock
Nocodazole
38.9
61.1
55.1
44.9
SSC
FL-1(GFP)
GFP-
GFP+
**
% of the cell
80
60
40
20
0
Mock
Noc

Figure 17. Survival advantage of Co- cultured iTPX2 cell under mitotic stress

(a) Survival advantage of iTPX2 cell was tested in different way. H9-P1-iTPX2 was co-cultured with same passaged H9-P1. Low dose of dox(0.1μg/ml) was treated, followed by nocodazole stress(20μg/ml)after 24hr. **(b)** After one week, GFP+ positive population become significantly increased in noc treated group compared to control group. n=6, unpaired, nonparametric t-test. p=0.0065. **(c)** Same experiment was done with eGFP tagged P1 and H9-iTPX2-#5. Cells were cultured under 20μg/ml of nocodazole stress without dox treatment. **(d)** eGFP negative population, in other words, iTPX2 cell line became dominant after one week. n=5, unpaired, nonparametric t-test. p=0.0043.

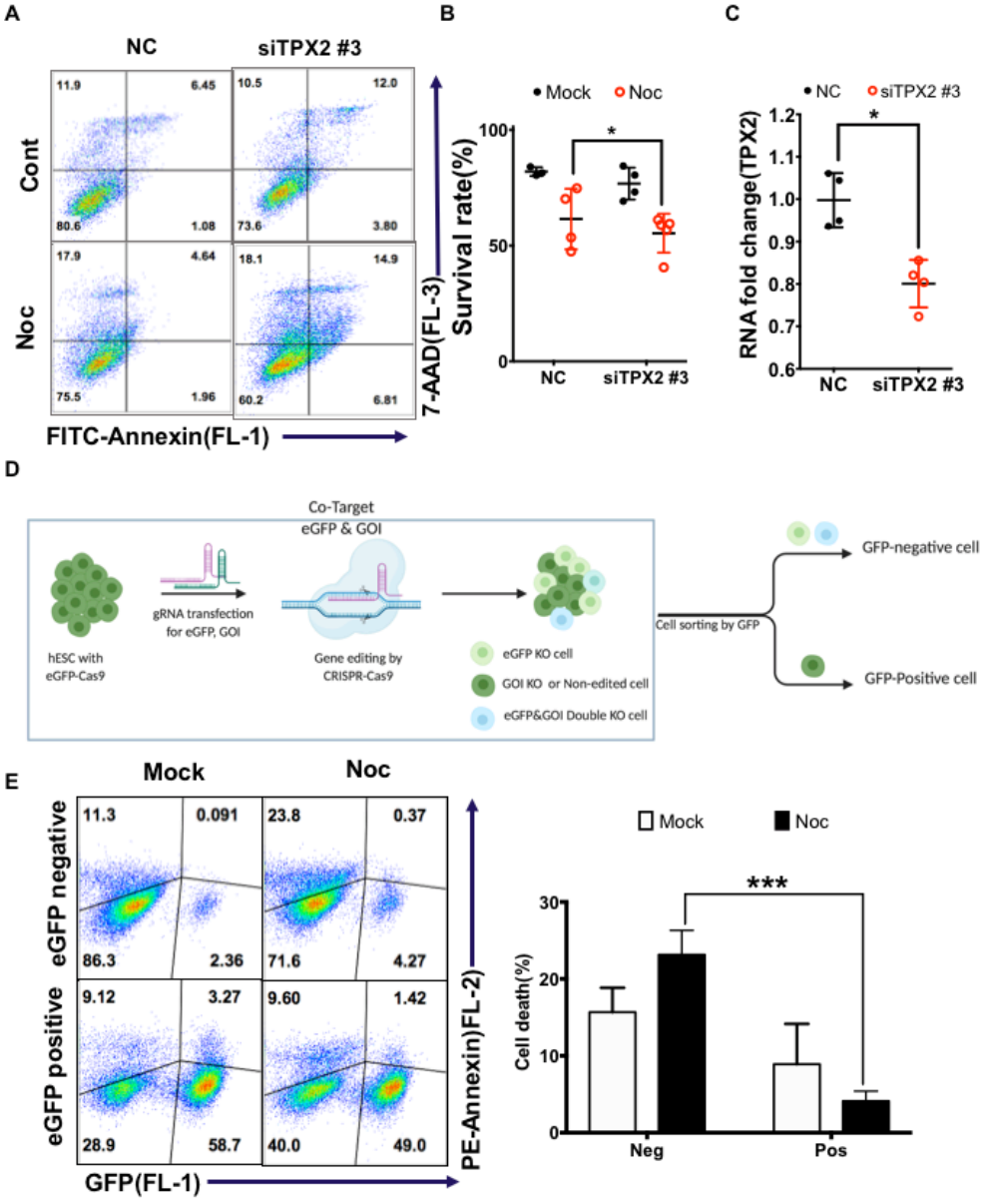
A
NC
siTPX2 #3
Cont
Noc
11.9
6.45
80.6
1.08
10.5
12.0
73.6
3.80
17.9
4.64
75.5
1.96
18.1
14.9
60.2
6.81
7-AAD(FL-3)
FITC-Annexin(FL-1)
B
Mock
Noc
Survival rate(%)
100
50
0
*
NC
siTPX2 #3
C
NC
siTPX2 #3
RNA fold change(TPX2)
1.2
1.1
1.0
0.9
0.8
0.7
0.6
*
NC
siTPX2 #3
D
Co-Target
eGFP & GOI
hESC with
eGFP-Cas9
gRNA transfection
for eGFP, GOI
Gene editing by
CRISPR-Cas9
eGFP KO cell
GOI KO or Non-edited cell
eGFP&GOI Double KO cell
Cell sorting by GFP
GFP-negative cell
GFP-Positive cell
E
Mock
Noc
eGFP negative
eGFP positive
11.3
0.091
86.3
2.36
23.8
0.37
71.6
4.27
9.12
3.27
28.9
58.7
9.60
1.42
40.0
49.0
PE-Annexin)FL-2)
GFP(FL-1)
Mock
Noc
***
Cell death(%)
30
20
10
0
Neg
Pos

Figure 18. Cell death by TPX2 depletion under mitotic stress

(a) Transient knockdown of TPX2 by siRNA reduces ability to resist against mitotic stress in P4. **(b)** Survival rate was quantified. Two-way ANOVA, n = 4, p =0.0275. **(c)** Knockdown efficacy was measured by mRNA level of TPX2. Unpaired nonparametric t-test, n=4, p=0.0286. **(d)** Co-targeting method for TPX2 KO was explained. After transfection of two guide RNA, for eGFP and GOI, sorting of eGFP negative population increases gene editing efficacy. **(e)** After co-targeting and sorting, ability to resist nocodazole stress was tested. eGFP negative population shows increased cell death compared to positive group under nocodazole stress. Two-way ANOVA, n=4, p=0.0004.

5. YAP1 stabilization via TPX2/AURKA axis for survival under mitotic stress

Even TPX2 is now proved to be a regulator of survival advantage during mitosis, exact mechanism is remained unclear. However, an importance of TPX2-AURKA axis in P4 was predicted based on RNA-seq of P1/P4 pair as displayed in Fig. 12. AURKA, a druggable target for genetically unstable cancer[51], cause multinucleation concomitant with amplification of centrosome when inducted, especially in p53 null mutation[52]. But paradoxically, inhibition of AURKA reported to be a inducer of mitotic abnormalities and aneuploidy in cancer [53]. Although, AURKA is not only required for spindle pole clustering centrosome maturation[54] but also in generation of extra centrosome[55]. Hence, AURKA and its stabilizer TPX2[44], is possible candidate as a driver of culture adaptation in hESCs, including H9, which are generally p53 mutant cell[22].

To examine prediction of major role of TPX2-AURKA axis in culture adaptation, early passage P1 and late passage P4 was treated with MLN8237(Alisertib), an inhibitor of Aurora kinase A/B[56]. Activity of Aurora Kinase A is high in P4, and 500nM of MLN8237 was enough for inhibition of phosphorylation, but still high than P1 (Fig.19A). MLN8237

relatively reduce survival under mitotic stress induced by nocodazole only in P4, thus cell death in P1 was not effected with or without MLN8237 (Fig. 19B). MLN8237 also significantly increases subG1 population as indicated in Fig. 19C. This result indicates importance of TPX2-AURKA axis in survival of P4.

For mechanistic study, I focused YAP (Yes-associated protein)/TAZ regulation. YAP/TAZ nexus is regulator of cellular proliferation, differentiation, and tissue homeostasis, controlled by both intrinsic and extrinsic stimuli, and likely critical for liking this changes to cell cycle progression[57]. AURKA, up-regulated in culture adapted hESCs, activates YAP signaling[58], and increase stability[59]. To examine relationship of TPX2-AURKA axis and YAP, H9-iTPX2 cell was used. Induction of TPX2 by treating doxycycline results in activation of AURKA (Fig. 20A), and also protein level of YAP(Fig. 20B). Hence, TPX2 affects to protein level of YAP is unexpected. Protein level of YAP increased in dox dose dependent manner as shown in Fig. 20C, with no difference in mRNA level (Fig. 20D).

However, we could not exclude the possibility that activation of YAP1 in T119, S289 and S367 during G2/M by cell cycle kinase CDK1[60] positively associated to protein stability. TPX2 are generally highly upregulated at G2/M phase[44], and excess TPX2 results in G0 arrest in prostate tumor cell line[61]

or G2/M arrest under long term treatment or high concentration of Dox as shown in Fig.14 in hESC-H9. Still, low dose of doxycycline gives moderate effects on cellular growth as shown on Fig.14B, and phosphorylation of YAP1 during mitosis differs from general inhibitory phosphorylation as S127 and S381 induced by Lats1/2 kinases which affects to stability of YAP1.

Knock down of TPX2 results decrease of phosphorylation of AURKA and protein level of YAP without phosphorylation differentiation. Intriguingly, protein level of YAP1 and TAZ, was decreased by KD of TPX2, compared to control group. YAP and TAZ are constant in second row, that siRNA treated but failed to maintain KD population due to lethality of high efficacy of knockdown of TPX2 (Fig. 20E). Increased protein stability of YAP1 in P4(Fig. 20F) was repeated by protein degradation test by inhibition of protein synthesis by cycloheximide under 0.1 doxycycline inducible TPX2 cell line, shows the result that YAP1 degradation was delayed under high level of TPX2 induced by doxycycline (Fig. 20G).

Culture adapted P4 shows increase mRNA level of TPX2 and BCL2L1, as indicated previously (Fig. 21A). Also, BIRC5(survivin), known as downstream gene of YAP1[57], is upregulated in P4. Consistent with result that TPX2-AURKA axis stabilize YAP, P4 shows increased YAP activity, tested by 8xGTIIC-luciferase (Fig. 21B). Activity of Wnt signaling was

downregulated in P4 tested by luciferase assay(Fig. 21C), allows to exclude alternative effect of Wnt signaling on culture adaptation as regulation of YAP/TAZ-TEAD pathway[62], and Wnt/β-catenin signaling via forming transcriptional complex with YAP[63].

By this results, YAP/TAZ-TEAD was emerged as the most promising candidate of survival regulation in culture adapted hESCs. Consistent with the hypothesis, an increase in the protein level of TEAD4 (Fig. 21D) and a decrease in phosphorylation of YAP were observed in P4 (Fig. 20E). Localization of YAP1 and TEAD4 is significantly high in nucleus of P4 (Fig. 21F), with other YAP downstream gene CTGF (Fig.21G)was increased. Localization of YAP1 is known to be most increased in G1 phase, while reduced during G2/M[64]. Hence, increasement of nuclear localization of YAP would not result from cell cycle, as length of G1 of P1 and P4 is not significantly different (Fig. 11E).

To examine role of YAP/TAZ-TEAD signaling pathway in regulation of survival, I discovered mRNA expression relationship in cancer patient data published in cBioportal. Interestingly, TEAD4 expression, conducting transcriptional complex with YAP1, was positively correlated with TPX2 expression in cancer cell line according to data provided from cBioportal as shown in Fig.22A. Overexpression of YAP1 significantly increase mRNA

level of BCL2Ll and CTGF (Fig. 22B), and TEAD4 also seen to serve role in expression of BCL2L1 as overexpression of TEAD4 increases mRNA level of BCL2L1 (Fig.22C). Knockdown of YAP (Fig.22D), TEAD4(Fig.22E), and TAZ(Fig. 22F) induce defect of BCL2L1 in mRNA level. As shown relationship between YAP/TAZ-TEAD axis and regulation of BCL2L1 in hESCs, we suggest that increased stability of YAP1 via TPX2-AURKA axis contributes to additional increasement of BCL2L1 in culture adapted hESCs, as driver of chromosomal abnormaligties.

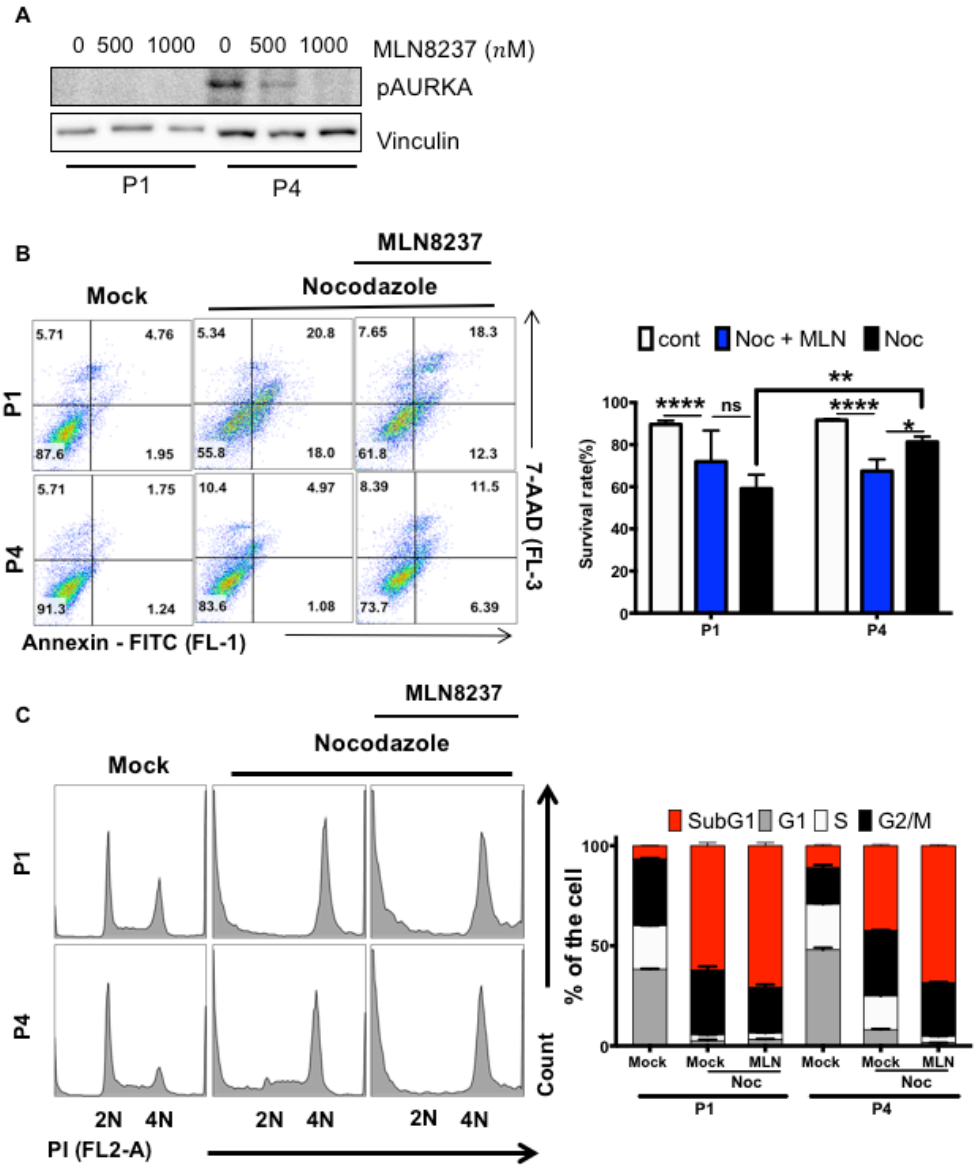
A
0 500 1000 0 500 1000 MLN8237 (nM)
pAURKA
Vinculin
P1
P4
B
MLN8237
Mock
Nocodazole
P1
P4
5.71
4.76
87.6
1.95
5.34
20.8
55.8
18.0
7.65
18.3
61.8
12.3
5.71
1.75
91.3
1.24
10.4
4.97
83.6
1.08
8.39
11.5
73.7
6.39
7-AAD (FL-3
Annexin - FITC (FL-1)
cont
Noc + MLN
Noc
Survival rate(%)
****
ns
**
****
*
P1
P4
C
MLN8237
Mock
Nocodazole
P1
P4
2N 4N
2N 4N
2N 4N
PI (FL2-A)
Count
SubG1
G1
S
G2/M
% of the cell
Mock
Mock
MLN
Noc
Mock
Mock
MLN
Noc
P1
P4

Figure 19. Abrogation of Mitotic survival by Aurora A inhibition

(a) Treatment of MLN8237 (Alisertib) decreases active phosphorylation of AURKA. **(b)** Co-treatment of MLN8237 and nocodazole decreases survival advantage in P4, while P1 showed no difference in survival. Two-way ANOVA, P1 Noc VS P4 Noc $p = 0.0011$, P1 Noc Vs Noc+MLN = ns, P1 Cont Vs Noc+MLN <0.0001, P4 Cont VS Noc+MLN $p<0.0001$, P4 Noc Vs Noc+MLN $p = 0.0177$. **(c)** Experiment repeated to test cell cycle by PI staining. As same with above, subG1 population of P4 increases when MLN8237 co treated with nocodazole.

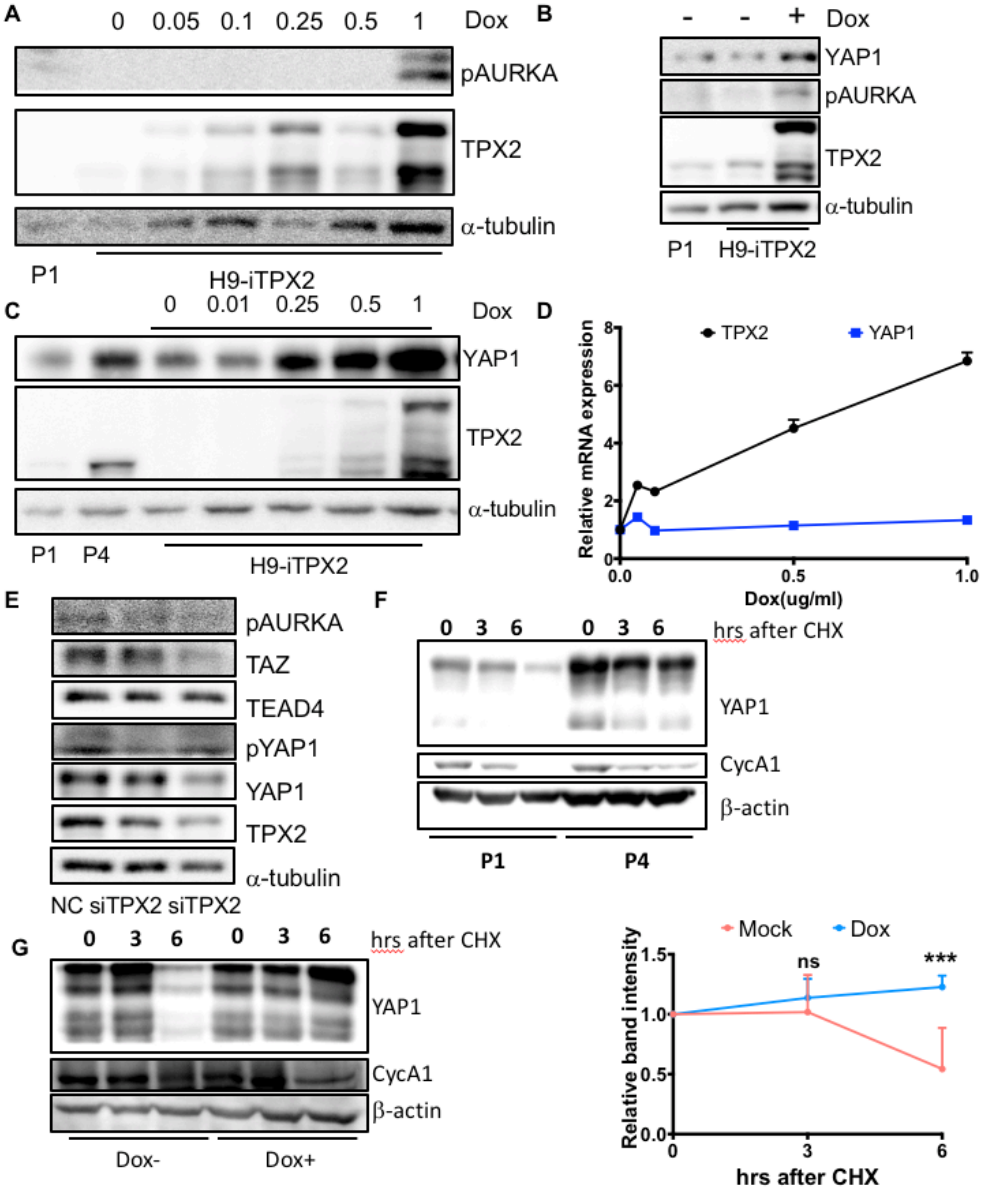
A
0 0.05 0.1 0.25 0.5 1 Dox
pAURKA
TPX2
α-tubulin
P1
H9-iTPX2
B
- - + Dox
YAP1
pAURKA
TPX2
α-tubulin
P1 H9-iTPX2
C
0 0.01 0.25 0.5 1 Dox
YAP1
TPX2
α-tubulin
P1 P4
H9-iTPX2
D
TPX2
YAP1
Relative mRNA expression
Dox(ug/ml)
E
pAURKA
TAZ
TEAD4
pYAP1
YAP1
TPX2
α-tubulin
NC siTPX2 siTPX2
F
0 3 6 0 3 6 hrs after CHX
YAP1
CycA1
β-actin
P1
P4
G
0 3 6 0 3 6 hrs after CHX
YAP1
CycA1
β-actin
Dox-
Dox+
Mock
Dox
ns
***
Relative band intensity
hrs after CHX

Figure 20. TPX2/AURKA axis for stabilization of YAP1

(a) Increased level of TPX2, induced by doxycycline, induces phosphorylation of AURKA in dose dependent manner. **(b)** Protein level of YAP1 increases after 0.1μg/ml of Dox treatment compared to untreated iTPX2 cell and P1. **(c)** Protein level of YAP1 increased in dox dose dependent manner, compared to P1 and P4. **(d)** High dose of doxycycline increases mRNA level of TPX2, but do not cause induction of YAP1 in mRNA level. **(e)** In compare of first and latest row, TPX2 KD cause decrease of active phosphorylation of AURKA and protein level of YAP1, TAZ. **(f-g)** For cycloheximide assay, 4hrs pre-treatment of 0.1μg/ml of doxycycline was exchanged to experimental media with constant dose of doxycycline. **(f)** P4 showed increased YAP1 stability. **(g)** Excess TPX2 induced by doxycycline reduce degradation of protein under cycloheximide treatment. Two-way ANOVA, n=4. p=0.0005 for 6hr.

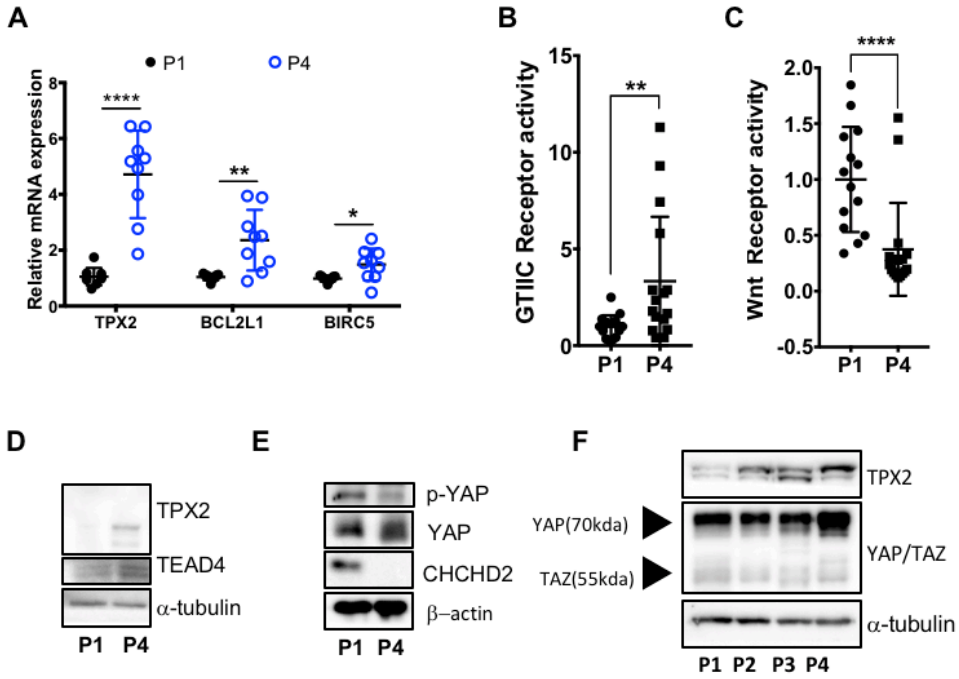
A
P1
P4
Relative mRNA expression
****
**
*
TPX2
BCL2L1
BIRC5
B
GTIIC Receptor activity
**
P1
P4
C
Wnt Receptor activity
****
P1
P4
D
TPX2
TEAD4
α-tubulin
P1 P4
E
p-YAP
YAP
CHCHD2
β–actin
P1 P4
F
YAP(70kda)
TAZ(55kda)
TPX2
YAP/TAZ
α-tubulin
P1 P2 P3 P4
G
TEAD4
YAP1
PARP
CHCHD2
α-tubulin
P1 P4
P1 P4
Cytosol
P1 P4
Nucleus

Figure 21. High YAP1 activity in P4

(a)mRNA level of BIRC5, a downstream gene of YAP1, was significantly high in P4. Nonparametric, unpaired t-test, n=9. $p<0.0001$ for TPX2, $p=0.0028$ for BCL2L1, and $p=0.0152$ for BIRC5. **(b)** 8X GTIIC reporter assay confirms high activity of YAP1 in P4. Nonparametric, unpaired t-test, n=16, $p=0.0051$. **(c)** Wnt signaling was high in P1, according to luciferase reporter assay. Nonparametric, unpaired t-test, n=14, $p<0.0001$. **(d)** Protein level of TEAD4 is high in P4, with TPX2. **(e)** Protein level of YAP1 is increased in P4, but phosphorylation was decreased. **(f)** TPX2, YAP gradually increases in protein level. **(g)** Nuclear localization of YAP1 is high in P4. **(h)** CTGF, a YAP1 downstream gene, is gradually increased proportionally with passage number.

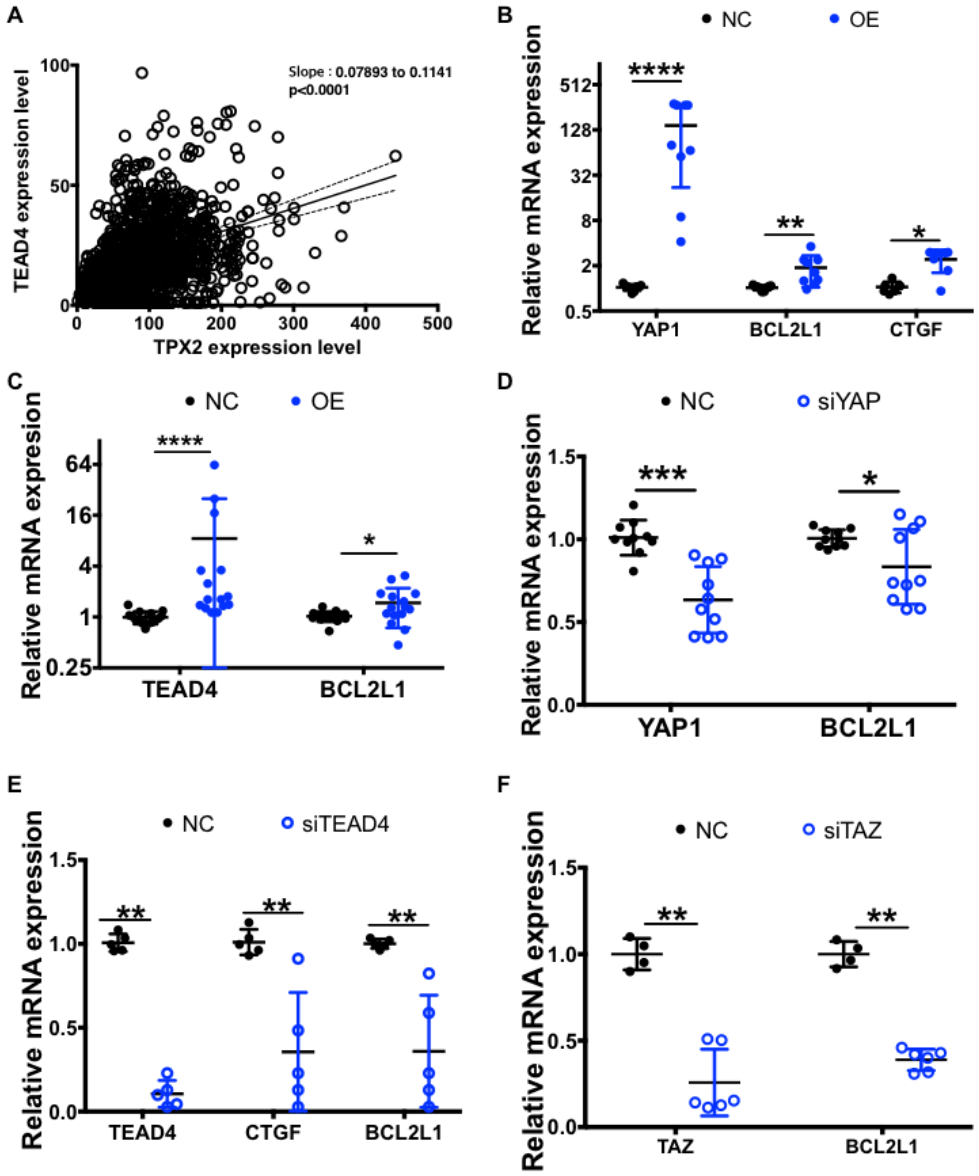
A
Slope : 0.07893 to 0.1141
p<0.0001
TEAD4 expression level
TPX2 expression level
B
NC
OE
Relative mRNA expression
YAP1
BCL2L1
CTGF
C
NC
OE
Relative mRNA expresion
TEAD4
BCL2L1
D
NC
siYAP
Relative mRNA expression
YAP1
BCL2L1
E
NC
siTEAD4
Relative mRNA expression
TEAD4
CTGF
BCL2L1
F
NC
siTAZ
Relative mRNA expression
TAZ
BCL2L1

Figure 22. Genetic perturbation of YAP/TAZ for BCL2L1 expression

(a) Expression of TPX2 and TEAD4 is positively correlated in lung cancer patient analyzed in cBioportal. n = 1376, Slope = 0.07893 to 0.1141(95% CI) **(b)** Overexpression of YAP1 results in increasement of BCL2L1. n= 9, unpaired t-test, parametric. $p<0.0001$ for YAP, $p=0.0082$ for BCl2L1, $p=0.0111$ for CTGF.**(c)** TEAD4 overexpression also occurs increased mRNA level of BCL2L1. n=15 unpaired t-test, nonparametric $p<0.0001$ for TEAD4, $p=0.0186$ for BCL2L1. **(d)** Decrease of YAP1 by siRNA diminish mRNA level of BCL2L1. n = 10, unpaired t-test, parametric. $p= 0.0002$ for YAP1, $p=0.0311$ for BCL2L1. **(e)**TEAD4 KD cell shows decreased CTGF and BCL2L1 mRNA level. n = 6 unpaired t-test, nonparametric. $p=0.0022$ for TEAD4, $p=0.0022$ for CTGF, $p=0.0022$ for BCL2L1. **(f)** TAZ KD also correlated with decreased mRNA level of BCL2L1. n = 4 for NC, 6 for siTAZ. Unpaired t-test, nonparametric. $P=0.0095$ for TAZ, $p=0.0095$ for BCL1L1.

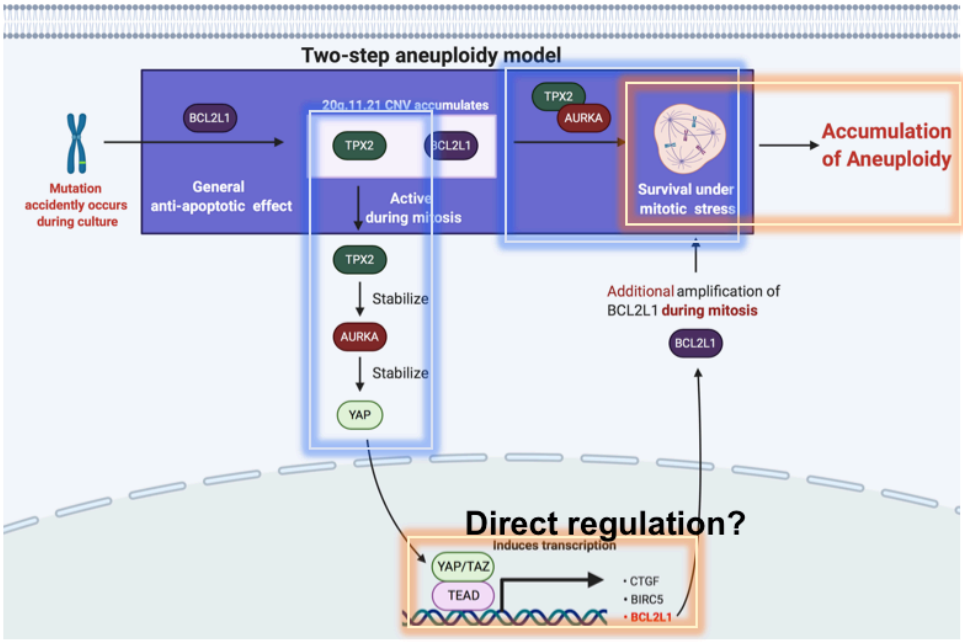

Figure 23. Scheme of TPX2/AURKA – YAP1 axis as survival regulator under mitotic stress

TPX2/AURKA axis is a driver of genetic alteration in hESCs, by induces survival advantage under mitotic stress. Overexpression of TPX2 gives resistance to early passage hESCs, while loss of TPX2 decreases survival advantage of late passage hESCs under mitotic stress. TPX2/AURKA axis stabilizes YAP1, showing strong correlation with translation of BCL2L1.

Discussion

Genetic aberration is a risk factor of clinical applications of PSCs

In contrast of potential of hPSCs as unlimited cellular source for regenerative therapies, risk factors of stem cell therapies discovered lately. Tumorigenicity according to genetic integrity is one of the three major risk[3], that accidently happens mutations selected and become dominant based on survival advantage during culture[10]. Driver for selection during culture adapted hESCs have been discovered, as induction of BCL2L1[21] and p53 mutation [22]gives strong survival advantage. Hence, CNV including 20q11.21 loci occurs even in the early passage [23], the incidence of abnormal karyotype may take prolong culture[24]. However, there are no clues for driver mutation that initiates chromosomal abnormality. Thus, additional mechanisms, that initiate genetic alteration, needed to be discovered for maintaining hESCs in genetically stable condition. If the cause of genetic alteration in human ESCs can be identified, it may be possible to prevent it or eliminate it before it manifests as a change in the chromosome.

TPX2 is a potent driver of genetic aberration

To answer the question in chromosome abnormality, we used isogenic pair model of four different passaged hESCs. By informatic analysis, we suggest TPX2 as strong candidate of driver for loss of genetic integrity. Our work reveals that TPX2, the regulator of mitosis with Aurora Kinase A, is a key regulator of initiation of genetic alteration due to induced survival advantage under mitotic stress. TPX2 is localized in 20q11.21 locus with BCL2L1[19], and increased during culture not only in mRNA but also protein level without cell cycle effect(Fig. 11). TPX2/AURKA axis is also predicted as desperate for survival of culture adapted hESCs (Fig. 12). Gain of TPX2 in doxycycline dependent transient expression clearly shows increasement of TPX2 is needed for survival under mitotic stress (Fig. 15, 16) without cell cycle arrest effect, while depletion of TPX2 leads to loss of survival ability of P4 under mitotic stress (Fig. 17, 18). By knowing that the TPX2/AURKA axis is important for culture adaptation, and inhibition of AURKA can serve as selective killer of culture adapted P4(Fig. 19), targeting TPX2/AURKA axis for selective elimination arose as a good strategy to make the pool of hESCs more suitable for clinical applications.

Role of TPX2/AURKA-YAP1 axis in culture adaptation of hESCs

Furthermore, it was found that the activation of AURKA caused by an increase in TPX2 stabilizes YAP1(Fig.20). Culture adapted hESCs, P4, not only showed high expression of downstream gene of YAP1, but also showed that the overall activity was high as observed through reporter assay(Fig. 21). Nuclear localization of YAP1 supports the result in which constantly high YAP1 activity in P4 compared to P1. This study also found that YAP1/TAZ-TEAD4 in hESCs has an effect on regulating the mRNA level of BCL2L1(Fig.22). Until now, it was widely known that BCL2L1 is important for the survival of hESCs. However, the precise regulatory mechanism is unknown. Further research is needed for mechanisms in regulation of stability and activity of YAP1.

In summary, our results suggest that TPX2/AURKA pathway, which is important for culture-adapted hESCs, is positively associated with transcription regulation of BCL2L1 via contribution of stabilizing YAP1.

Bibliography

1. Ilic D, Ogilvie C. Concise Review: Human Embryonic Stem Cells—What Have We Done? What Are We Doing? Where Are We Going? Stem Cells. 2017;35:17–25.

2. Thomson JA. Embryonic stem cell lines derived from human blastocysts. Science (80-). 1998;282:1145–7.

3. Heslop JA, Hammond TG, Santeramo I, Tort Piella A, Hopp I, Zhou J, et al. Concise Review: Workshop Review: Understanding and Assessing the Risks of Stem Cell-Based Therapies. Stem Cells Transl Med. 2015;4:389–400.

4. AS Lee et al, Chad Tang, Mahendra S. Rao, Irving L. Weissman and JC, Wu. Tumorigenicity as a Clinical Hurdle for Pluripotent Stem Cell Therapies. Nat Med. 2013;8:998–1004.

5. Blum B, Benvenisty N. The tumorigenicity of diploid and aneuploid human pluripotent stem cells. Cell Cycle. 2009;8:3822–30.

6. Maitra A, Arking DE, Shivapurkar N, Ikeda M, Stastny V, Kassauei K, et al. Genomic alterations in cultured human embryonic stem cells. Nat Genet. 2005;37:1099–103.

7. Garber K. RIKEN suspends first clinical trial involving induced pluripotent stem cells. Nat Biotechnol. Nature Publishing Group; 2015;33:890–1.

8. Halliwell J, Barbaric I, Andrews PW. Acquired genetic changes in human pluripotent stem cells: origins and consequences. Nat Rev Mol Cell Biol

[Internet]. Springer US; 2020;1–14. Available from: http://www.nature.com/articles/s41580-020-00292-z
9. Baker DEC, Harrison NJ, Maltby E, Smith K, Moore HD, Shaw PJ, et al. Adaptation to culture of human embryonic stem cells and oncogenesis in vivo. Nat Biotechnol. 2007;25:207–15.
10. Ben-David U, Arad G, Weissbein U, Mandefro B, Maimon A, Golan-Lev T, et al. Aneuploidy induces profound changes in gene expression, proliferation and tumorigenicity of human pluripotent stem cells. Nat Commun. Nature Publishing Group; 2014;5:1–11.
11. Ben-David U, Benvenisty N. The tumorigenicity of human embryonic and induced pluripotent stem cells. Nat Rev Cancer. Nature Publishing Group; 2011;11:268–77.
12. Cimini D, Howell B, Maddox P, Khodjakov A, Degrassi F, Salmon ED. Merotelic kinetochore orientation is a major mechanism of aneuploidy in mitotic mammalian tissue cells. J Cell Biol. 2001;152:517–27.
13. Dreesen O, Brivanlou AH. Signaling pathways in cancer and embryonic stem cells. Stem Cell Rev. 2007;3:7–17.
14. Ben-David U. Genomic instability, driver genes and cell selection: PROJECTIONS from cancer to stem cells. Biochim Biophys Acta - Gene Regul Mech. 2015;1849:427–35.
15. Tosca L, Feraud O, Magniez A, Bas C, Griscelli F, Bennaceur-Griscelli A, et al. Genomic instability of human embryonic stem cell lines using different passaging culture methods. Mol Cytogenet [Internet]. ???; 2015;8:1–11. Available from: ???
16. Liu JC, Guan X, Ryan JA, Rivera AG, Mock C, Agarwal V, et al. High mitochondrial priming sensitizes hESCs to DNA-damage-induced apoptosis.

Cell Stem Cell [Internet]. Elsevier Inc.; 2013;13:483–91. Available from: http://dx.doi.org/10.1016/j.stem.2013.07.018
17. Peterson SE, Loring JF. Genomic instability in pluripotent stem cells: Implications for clinical applications. J Biol Chem. 2014;289:4578–84.
18. Mayshar Y, Ben-David U, Lavon N, Biancotti JC, Yakir B, Clark AT, et al. Identification and classification of chromosomal aberrations in human induced pluripotent stem cells. Cell Stem Cell [Internet]. Elsevier Inc.; 2010;7:521–31. Available from: http://dx.doi.org/10.1016/j.stem.2010.07.017
19. Lefort N, Feyeux M, Bas C, Féraud O, Bennaceur-Griscelli A, Tachdjian G, et al. Human embryonic stem cells reveal recurrent genomic instability at 20q11.21. Nat Biotechnol. 2008;26:1364–6.
20. Biancotti JC, Benvenisty N. Aneuploid human embryonic stem cells: Origins and potential for modeling chromosomal disorders. Regen Med. 2011;6:493–503.
21. Avery S, Hirst AJ, Baker D, Lim CY, Alagaratnam S, Skotheim RI, et al. BCL-XL mediates the strong selective advantage of a 20q11.21 amplification commonly found in human embryonic stem cell cultures. Stem Cell Reports [Internet]. Elsevier; 2013;1:379–86. Available from: http://dx.doi.org/10.1016/j.stemcr.2013.10.005
22. Merkle FT, Ghosh S, Kamitaki N, Mitchell J, Avior Y, Mello C, et al. Human pluripotent stem cells recurrently acquire and expand dominant negative P53 mutations. Nature. 2017;545:229–33.
23. Martins-Taylor K, Nisler BS, Taapken SM, Compton T, Crandall L, Montgomery KD, et al. Recurrent copy number variations in human induced pluripotent stem cells. Nat Biotechnol. 2011;29:488–91.

24. Närvä E, Autio R, Rahkonen N, Kong L, Harrison N, Kitsberg D, et al. High-resolution DNA analysis of human embryonic stem cell lines reveals culture-induced copy number changes and loss of heterozygosity. Nat Biotechnol. 2010;28:371–7.
25. Aguilera A, Gómez-González B. Genome instability: A mechanistic view of its causes and consequences. Nat Rev Genet. 2008;9:204–17.
26. Zhang J, Hirst AJ, Duan F, Qiu H, Huang R, Ji Y, et al. Anti-apoptotic Mutations Desensitize Human Pluripotent Stem Cells to Mitotic Stress and Enable Aneuploid Cell Survival. Stem Cell Reports. 2019;12:557–71.
27. Burrell RA, McClelland SE, Endesfelder D, Groth P, Weller MC, Shaikh N, et al. Replication stress links structural and numerical cancer chromosomal instability. Nature. Nature Publishing Group; 2013;494:492–6.
28. Bird AW, Hyman AA. Building a spindle of the correct length in human cells requires the interaction between TPX2 and Aurora A. J Cell Biol. 2008;182:289–300.
29. Neumayer G, Belzil C, Gruss OJ, Nguyen MD. TPX2: Of spindle assembly, DNA damage response, and cancer. Cell Mol Life Sci. 2014;71:3027–47.
30. Aguirre-Portolés C, Bird AW, Hyman A, Cañamero M, Pérez De Castro I, Malumbres M. Tpx2 controls spindle integrity, genome stability, and tumor development. Cancer Res. 2012;72:1518–28.
31. Naso FD, Sterbini V, Crecca E, Asteriti IA, Russo AD, Giubettini M, et al. Excess TPX2 Interferes with Microtubule Disassembly and Nuclei Reformation at Mitotic Exit. Cells. 2020;9:374.

32. Sillars-Hardebol AH, Carvalho B, Tijssen M, Beliën JAM, De Wit M, Delis-van Diemen PM, et al. TPX2 and AURKA promote 20q amplicon-driven colorectal adenoma to carcinoma progression. Gut. 2012;61:1568–75.
33. Carter SL, Eklund AC, Kohane IS, Harris LN, Szallasi Z. A signature of chromosomal instability inferred from gene expression profiles predicts clinical outcome in multiple human cancers. Nat Genet. 2006;38:1043–8.
34. Chen Q, Cao B, Nan N, Wang Y, Zhai X, Li Y, et al. TPX2 in human clear cell renal carcinoma: Expression, function and prognostic significance. Oncol Lett. 2016;11:3515–21.
35. Barbaric I, Biga V, Gokhale PJ, Jones M, Stavish D, Glen A, et al. Time-lapse analysis of human embryonic stem cells reveals multiple bottlenecks restricting colony formation and their relief upon culture adaptation. Stem Cell Reports [Internet]. The Authors; 2014;3:142–55. Available from: http://dx.doi.org/10.1016/j.stemcr.2014.05.006
36. Cho SJ, Kim KT, Jeong HC, Park JC, Kwon OS, Song YH, et al. Selective Elimination of Culture-Adapted Human Embryonic Stem Cells with BH3 Mimetics. Stem Cell Reports [Internet]. ElsevierCompany.; 2018;11:1244–56. Available from: https://doi.org/10.1016/j.stemcr.2018.09.002
37. Jo HY, Lee Y, Ahn H, Han HJ, Kwon A, Kim BY, et al. Functional in vivo and in vitro effects of 20q11.21 genetic aberrations on hPSC differentiation. Sci Rep [Internet]. Nature Publishing Group UK; 2020;10:1–14. Available from: https://doi.org/10.1038/s41598-020-75657-7
38. Amps K, Andrews PW, Anyfantis G, Armstrong L, Avery S, Baharvand H, et al. Screening ethnically diverse human embryonic stem cells identifies

a chromosome 20 minimal amplicon conferring growth advantage. Nat Biotechnol. 2011;29:1132–44.
39. Krämer A, Maier B, Bartek J. Centrosome clustering and chromosomal (in)stability: A matter of life and death. Mol Oncol. 2011;5:324–35.
40. Castle JC, Loewer M, Boegel S, Tadmor AD, Boisguerin V, De Graaf J, et al. Mutated tumor alleles are expressed according to their DNA frequency. Sci Rep. 2014;4:1–6.
41. Lee MO, Moon SH, Jeong HC, Yi JY, Lee TH, Shim SH, et al. Inhibition of pluripotent stem cell-derived teratoma formation by small molecules. Proc Natl Acad Sci U S A. 2013;110:1–10.
42. Romero-Lanman EE, Pavlovic S, Amlani B, Chin Y, Benezra R. Id1 maintains embryonic stem cell self-renewal by up-regulation of nanog and repression of brachyury expression. Stem Cells Dev. 2012;21:384–93.
43. Alfaro-Aco R, Thawani A, Petry S. Structural analysis of the role of TPX2 in branching microtubule nucleation. J Cell Biol. 2017;216:983–97.
44. Giubettini M, Asteriti IA, Scrofani J, De Luca M, Lindon C, Lavia P, et al. Control of Aurora-A stability through interaction with TPX2. J Cell Sci. 2011;124:113–22.
45. Kufer TA, Silljé HHW, Körner R, Gruss OJ, Meraldi P, Nigg EA. Human TPX2 is required for targeting Aurora-A kinase to the spindle. J Cell Biol. 2002;158:617–23.
46. Lee DF, Su J, Ang YS, Carvajal-Vergara X, Mulero-Navarro S, Pereira CF, et al. Regulation of embryonic and induced pluripotency by aurora kinase-p53 signaling. Cell Stem Cell. 2012;11:179–94.
47. Asteriti IA, Rensen WM, Lindon C, Lavia P, Guarguaglini G. The Aurora-A/TPX2 complex: A novel oncogenic holoenzyme? Biochim

Biophys Acta - Rev Cancer [Internet]. Elsevier B.V.; 2010;1806:230–9. Available from: http://dx.doi.org/10.1016/j.bbcan.2010.08.001
48. Ding L, Zhang S, Chen S, Zheng L, Xiao L. Effect and mechanism of lentivirus-mediated silencing of TPX2 gene on proliferation and apoptosis of human hepatoma cells. J Cell Biochem. 2019;120:8352–8.
49. Mali P, Yang L, Esvelt KM, Aach J, Guell M, DiCarlo JE, et al. RNA-guided human genome engineering via Cas9. Science (80-). 2013;339:823–6.
50. Kim KT, Park JC, Jang HK, Lee H, Park S, Kim J, et al. Safe scarless cassette-free selection of genome-edited human pluripotent stem cells using temporary drug resistance. Biomaterials [Internet]. Elsevier Ltd; 2020;262:120295. Available from: https://doi.org/10.1016/j.biomaterials.2020.120295
51. van Gijn SE, Wierenga E, van den Tempel N, Kok YP, Heijink AM, Spierings DCJ, et al. TPX2/Aurora kinase A signaling as a potential therapeutic target in genomically unstable cancer cells. Oncogene [Internet]. Springer US; 2019;38:852–67. Available from: http://dx.doi.org/10.1038/s41388-018-0470-2
52. Meraldi P, Honda R, Nigg EA. Aurora-A overexpression reveals tetraploidization as a major route to centrosome amplification in p53-/- cells. EMBO J. 2002;21:483–92.
53. Asteriti IA, Cesare E Di, Mattia F De, Hilsenstein V, Neumann B, Cundari E, et al. The Aurora-A inhibitor MLN8237 affects multiple mitotic processes and induces dose-dependent mitotic abnormalities and aneuploidy. Oncotarget. 2014;5:6229–42.

54. Barr AR, Gergely F. Aurora-A: The maker and breaker of spindle poles. J Cell Sci. 2007;120:2987–96.
55. Navarro-Serer B, Childers EP, Hermance NM, Mercadante D, Manning AL. Aurora A inhibition limits centrosome clustering and promotes mitotic catastrophe in cells with supernumerary centrosomes. Oncotarget. 2019;10:1649–59.
56. Niu H, Manfredi M, Ecsedy JA. Scientific rationale supporting the clinical development strategy for the investigational Aurora A kinase inhibitor alisertib in cancer. Front Oncol. 2015;5:1–9.
57. Hansen CG, Moroishi T, Guan KL. YAP and TAZ: A nexus for Hippo signaling and beyond. Trends Cell Biol [Internet]. Elsevier Ltd; 2015;25:499–513. Available from: http://dx.doi.org/10.1016/j.tcb.2015.05.002
58. Chang SS, Yamaguchi H, Xia W, Lim SO, Khotskaya Y, Wu Y, et al. Aurora A kinase activates YAP signaling in triple-negative breast cancer. Oncogene. 2017;36:1265–75.
59. Wang P, Gong Y, Guo T, Li M, Fang L, Yin S, et al. Activation of Aurora A kinase increases YAP stability via blockage of autophagy. Cell Death Dis [Internet]. Springer US; 2019;10. Available from: http://dx.doi.org/10.1038/s41419-019-1664-4
60. Yang S, Zhang L, Liu M, Chong R, Ding SJ, Chen Y, et al. CDK1 phosphorylation of YAP promotes mitotic defects and cell motility and is essential for neoplastic transformation. Cancer Res. 2013;73:6722–33.
61. Zou J, Huang RY, Jiang FN, Chen DX, Wang C, Han ZD, et al. Overexpression of TPX2 is associated with progression and prognosis of prostate cancer. Oncol Lett. 2018;16:2823–32.

62. Park HW, Kim YC, Yu B, Moroishi T, Mo JS, Plouffe SW, et al. Alternative Wnt Signaling Activates YAP/TAZ. Cell. 2015;162:780–94.
63. Rosenbluh J, Nijhawan D, Cox AG, Li X, Neal JT, Schafer EJ, et al. β-Catenin-driven cancers require a YAP1 transcriptional complex for survival and tumorigenesis. Cell [Internet]. Elsevier Inc.; 2012;151:1457–73. Available from: http://dx.doi.org/10.1016/j.cell.2012.11.026
64. Kim W, Cho YS, Wang X, Park O, Ma X, Kim H, et al. Hippo signaling is intrinsically regulated during cell cycle progression by APC/CCdh1. Proc Natl Acad Sci U S A. 2019;116:9423–32.

국문 초록

배양된 인간배아줄기세포(human embryonic stem cell, hESC)에서는 유전적 변이가 일어나는데, 이는 hESC 를 기반으로 한 치료에서 치명적인 안전성 문제를 야기할 수 있음에도 불구하고 이해된 바가 적다. 한편, 20q11.21 염색체에서 나타나는 유전자 복제 변이(Copy Number Variation, CNV)는 BCL2L1 의 증가를 통해 생존에 이점을 가져옴으로써 오랜 기간 배양했을 때 가장 흔히 발생하는 변이 중 하나다. 그러나 이 변이의 시작점(Driver)이 무엇인지는 알지 못하여, 우리는 여러 passage 의 ESC 를 사용해 이를 밝히고자 했다. 가장 오랫동안 배양된 세포(P4)는 유사분열 과정에서의 이상이 확연히 관찰되며, 20q11.21 좌위의 CNV 와 BCL2L1 의 증가로 인해 생존에 이점이 있음이 확인되었다. 20q11.21 에 위치하며 정상적인 유사분열 과정에서 방추사의 형성에 관여하는 한편, 암의 악성도에 영향을 미치는 유전자인 TPX2 는 이러한 기능을 고려할 때 hESC 에서도 유사분열 과정에 관여함으로서 결과적으로 유전적 이상을 야기하는 핵심 driver 일 가능성이 있다. 우리는 정상 세포에서 인위적으로 일정 기간 동안 TPX2 를 증가시켰을 때 유사분열 도중의 스트레스로부터 세포를 보호함을 확인했다. 후속 연구에서 보다 구체적인 작용 기작에 대해 밝힐 예정이다.

주요어 : TPX2, Survival advantage, hESCs, Aberrant mitosis, Genetic alteration

학번 : 2019-22260